EFFECT OF Zn:Se RATIO ON OPTICAL AND ELECTRICAL CHARACTERISTICS OF SPRAYED ZnSe THIN FILMS

M. Sc. Thesis

in

Engineering Physics
University of Gaziantep

By
Rıdvan ORMANCI

JULY 2006

ABSTRACT

EFFECT OF Zn:Se RATIO ON OPTICAL AND ELECTRICAL CHARACTERISTICS OF SPRAYED ZnSe THIN FILMS

ORMANCI, Rıdvan
M. Sc. in Engineering Physics
Supervisor: Asist. Prof. Dr. Metin BEDİR
July 2006, 59 Pages

In this study, semiconducting ZnSe thin films were developed under different Zn ratios by using spraying pyrolysis method and their optical and electrical properties were widely investigated by using different techniques.

The crystal structure of the ZnSe samples were determined from x-ray diffraction peaks and the thickness of the sprayed ZnSe thin film samples were calculated by using weighing method. The optical properties of semiconducting ZnSe thin films were investigated from optical absorption coefficient data using double beam visible spectrofotometer. By using these data band gap energies of the semiconducting ZnSe thin films were determined. The electrical properties of the ZnSe thin film samples were investigated by Vander Pauw method (four ohmic contact). The changes in the resistivities, conductivities and Hall Mobilities of the ZnSe thin film samples under different Zn ratios have been investigated.

Key words: Spray pyrolysis method, ZnSe thin film, Structural, optical and electrical properties.

ÖZET

PÜSKÜRTME YÖNTEMİYLE ELDE EDİLEN ZnSe İNCE FİLMLERİNİN OPTİKSEL VE ELEKTRİKSEL KARAKTERİSTİKLERİ ÜZERİNE Zn:Se ORANLARININ ETKİSİ

ORMANCI, Rıdvan
Master Tezi, Fizik Mühendisliği
Danışman: Yrd.Doç.Dr. Metin BEDİR
Temmuz 2006, 59 Sayfa

Bu çalışmada püskürtme yöntemiyle cam alt tabanlar üzerine farklı Zn oranlarında ZnSe ince filmler büyütülüp, onların yapısal, optiksel ve elektriksel özellikleri farklı teknikler kullanılarak derinlemesine araştırılmıştır. ZnSe ince film numunelerinin kristal yapıları x-ışınımı difraktometresinden elde edilen pikler kullanılarak incelenmiş ve ince film numunelerinin kalınlıkları ağırlık yöntemiyle hesaplanmıştır. Yarı iletken ZnSe ince filmlerin optiksel özellikleri çift ışıklı olup görünür bölgede çalışan spekrometreden elde edilen optiksel soğurma katsayıları analiziyle araştırılmıştır. Bu veriler kullanılarak yarı iletken ZnSe ince filmlerin enerji band değerleri hesaplanmıştır. ZnSe ince film numunelerinin elektriksel özellikleri Van der Pauw (dört nokta kontakt) metoduyla

incelenmiştir. Farklı Zn oranlarında elde edilen ZnSe ince filmlerinin özdirençleri, öziletkenlikleri ve Hall mobilitelerinin Zn oranına göre değişimi araştırılmıştır.

Anahtar kelimeler: Püskürtme yöntemi, ZnSe ince film, Yapısal, optiksel ve elektriksel özellikler.

ACKNOWLEDGEMENT

During the writing of this thesis, the author received many helps from people to whom he would like to thank. First of all I would like to thank my supervisor Assist. Prof. Dr. Metin BEDİR for all his help and advice during the preperation of this thesis. Secondly, I wish to thank Assist. Prof. Dr. Mustafa ÖZTAŞ .I have benefited from the aid and advice of him during the writing and preparation of this thesis. I am truly grateful for the encouragement and consideration of him. I would like to thank my gratitude to the research assistances and other personnel at the Department of Engineering Physics for their kind help and friendships. And also for their helps his primary school's staffs; manager; Ömer ÇAM and Ali ÇALI and co-managers; Ömer ARSLAN and Vahap ÖZKAN.

The author's special thanks go to his wife, Aysel ORMANCI and his sister; Ferdane ORMANCI.

TABLE OF CONTENTS

ABSTRACT	……………………………………………………....	iii
ÖZET	………………………………………………………	iv
ACKNOWLEDGMENT	……………………………………………………….	v
TABLE OF CONTENTS	……………………………………………………….	vi
LIST OF FIGURES	………………………………………………………	ix
LIST OF TABLES	……………………………………………………….	xii

CHAPTER	**1.**	**INTRODUCTION**……………………………………..	1
CHAPTER	**2.**	**THEORY OF SEMICONDUCTOR**……………….....	7
	2.1.	Semiconductor Materials…………………………………	7
	2.2.	Compound II-VI Semiconductors………………………	10
	2.3.	Band Theory of Solids…………………………………..	10
	2.4.	Semiconductor Band Structure…………………….……	12
	2.5.	Doping of semiconductors………………………………	13
	2.6.	Intrinsic and extrinsic semiconductors………………....	14
	2.6.1.	N-type doping……………………………………...…	14
	2.6.2.	P-type doping…………………………………………...	15

	2.7.	Direct transition and Indirect transition……………….....15	
	2.8.	Impurities……………………………………………..16	
	2.9.	Absorption Of Semiconducting Materials………………19	
	2.9.1.	Optical Absorption……………………………………...19	
	2.9.2.	Transmission And Absorption…………………………..20	
	2.9.3.	Absorption Constant and Band Gap…………………….21	
	2.10.	Hall Mobility……………………………………………24	
CHAPTER	**3.**	**EXPERIMENTAL STUDIES**………………………...28	
		THIN FILM PRODUCTION TECHNIQUES…..…..28	
	3.1.	Spray Pyrolysis Method…………………………...…28	
	3.1.1.	Introduction……………………………...………...28	
	3.1.2.	Experimental set-up of Spraying System…………...…28	
	3.1.3.	Deposition Apparatus…………………………………...29	
	3.2.	Growth mechanism of the semiconducting thin films by the spraying pyrolysis method…………………………..30	
	3.2.1.	Introduction……………………………………………..30	
	3.2.2.	Substrate Preparation……………………………………30	
	3.2.3.	Spraying Solution Preparation…………………………..31	
	3.2.4.	Development of ZnSe Thin Films………………………32	
CHAPTER	**4.**	**MEASUREMENTS AND RESULTS**………….........33	
	4.1.	TheThickness Determination of ZnSe Thin Films…..…33	
	4.2.	Optical studies……………………………………..…33	
	4.3.	The Crystal Structure of The Thin Film Samples………34	
	4.3.1.	X-Ray Diffraction Study..34	
	4.4.	Electrical Measurements..35	
	4.4.1.	Resistivity And Conductivity Measurements..................35	

4.4.2. Hall Mobility Measurements…………………………....36
4.5. Results and Discussion………………………………….37
4.5.1. The Thickness Determination of ZnSe Thin Films……..37
4.5.2. Optical Studies…………………………………………..37
4.5.3. X-Ray Diffraction……………………………………….42
4.5.4. Grain Size Studies……………………………………....43
4.5.5. Studies On Electrical Parameters……………………….45
4.5.6. Discussion……………………………………………….48

REFERANCES………………………………...........51

LIST OF FIGURES

Figure No		Page
Figure 2.1	Energy Bands for Solids	11
Figure 2.2	A band gap model in insulators and semiconductors	11
Figure 2.3	(**a**) Direct transition via photon absorbtion (**b**) Indirect transition via photon *and* phonon absorption (for momentum conservation)	16
Figure 2.4	Crystal lattice structure	17
Figure 2.5	Lattice structure of n-type material	18
Figure 2.6	Lattice structure of p-type material	19
Figure 2.7	Obtical absorbtion of a photon with hv > E_g :(a) an EHP is created during photon absorption; (b) the excited electron gives up energy to the lattice by scatterring events; (c) the electron recombines with a hole in the valence band	20
Figure 2.8	Optical absorption experiment	21
Figure 2.9	Optical absorption	
	(a) Semiconductor under illumination	22
	(b) Exponential decay of photon flux.	22

Figure 2.10 Band gaps of some common semiconductors relative to the optical spectrum 23

Figure 2.11 Hall Effect 25

Figure 3.1 Schematic diagram of the spray pyrolysis system 29

Figure 3.2 Cleaning process of the glass substrate 31

Figure 4.1 In-ohmic contacts prepared on thin film samples 35

Figure 4.2 Resistivity measurement set-up 35

Figure 4.3 The standart configuration used for hall effect measurement 36

Figure 4.4 Plot of $(\alpha h\nu)^2$ versus photon energy ($h\nu$) for film the Zn:Se (0,2:1) thin film grown by using spraying pyrolysis method 38

Figure 4.5 Plot of $(\alpha h\nu)^2$ versus photon energy ($h\nu$) for film the Zn:Se (0,4:1) thin film grown by using spraying pyrolysis method 38

Figure 4.6 Plot of $(\alpha h\nu)^2$ versus photon energy ($h\nu$) for film the Zn:Se (0,6:1) thin film grown by using spraying pyrolysis method 39

Figure 4.7 Plot of $(\alpha h\nu)^2$ versus photon energy ($h\nu$) for film the Zn:Se (0,8:1) thin film grown by using spraying pyrolysis method 39

Figure 4.8 Plot of $(\alpha h\nu)^2$ versus photon energy ($h\nu$) for film the Zn:Se (1:1) thin film grown by using spraying pyrolysis method 40

Figure 4.9 Plot of $(\alpha h\nu)^2$ versus photon energy ($h\nu$) for film the ZnSe thin films grown by using spraying pyrolysis method 41

Figure 4.10 Variation of the bandgap energy versus molar ratio of Zn. 42

Figure 4.11 X-ray diffraction patterns for different Zn:Se ratios: (a) 1:1; (b) 0.2:1; (c) 0.4:1; (d) 0.6:1; and (e) 0.8:1 43

Figure 4.12 The molar ratio of Zn versus the grain size 44

Figure 4.13 The molar ratio of Zn versus resistivity 46

Figure 4.14 The molar ratio of Zn versus the conductivity 47

Figure 4.15 The molar ratio of Zn versus the Hall Mobility 47

LIST OF TABLES

Table No		Page
Table 2.1	Common semiconductor materials: (a) the portion of the periodic table where semiconductors occur; (b) elemental and compound semiconductors	9
Table 4.1	The thickness of ZnSe thin film	37
Table 4.2	The band gap energy values of ZnSe thin films	40
Table 4.3	Grain size values of the ZnSe thin films with different Zn ratio	44
Table 4.4	The resistivity, conductivity and Hall Mobility values of ZnSe thin film samples	45

CHAPTER 1

INTRODUCTION

Binary semiconductors are considered as important technological materials because of their potential applications in optoelectronic devices, solar cells, IR detectors and lasers [1,2]. Binary compounds of group IIB and group VIA elements, commonly referred to as II-VI compounds, have technologically important applications. Among these compounds, only CdTe and ZnSe can be prepared in both n- and p-type forms [3]. The synthesis of II-VI semiconductors has been recently the focus of much attention for various optoelectronic applications, especially for blue light-emitting diodes and laser diodes [4-6]. It is known that the photoelectronic and other properties of II-VI class of compound thin films are highly structure sensitive which it turn can severely influence the device performance. The structure parameters; the crystallinity, crystal phase, lattice constant, average stress and strain, grain size orientation etc are strongly dependent on deposition parameters [7].

Thin films of ZnSe have attracted considerable interest over the years owing to their wide range of applications in various opto-electronic devices such as LED in short wavelength region, ultrasonic transducers, photodetectors and in solar cells. It has a direct band gap (2.68 eV) and is transparent over a wide range of visible spectrum. More progress has been achieved in fabrication of blue-green light emitting diodes, dielectric mirrors, filters and other optically sensitive devices [8,9].

ZnSe thin films have been usually grown by molecular beam epitaxy and chemical vapor deposition [10,11]. On the other hand, several reports on the electrodeposition from aqueous solutions [12,13] as well as from molten salts have been published. However, little study has been reported about the spray pyrolysis ZnSe thin films. The method of spray pyrolysis (or solution spraying) is a convenient and economical method for the growth of thin films for solar cell applications. Recently, this technique has been extensively studied by researchers, because spraying pyrolysis method is a simple for

the deposition of semiconductor films. This method is also economically attractive compared to the other fabrication methods.

The zinc selenide (ZnSe) thin films are deposited onto glass substrate using relatively simple and inexpensive successive ionic layer adsorption and reaction (SILAR) method. The X-ray diffraction (XRD) study and scanning electron microscopy (SEM) studies reveals nanocrystalline nature alongwith some amorphous phase present in ZnSe thin films. Room temperature deposition of ZnSe thin films on glass substrate is possible by SILAR method. The as-deposited ZnSe thin films are nanocrystalline along with amorphous phase present in it, while in annealed film amorphous phase is present with the polycrystalline cubic structure. The films are semiconducting in nature with room temperature electrical resistivity of the order of 10^7 V cm. Thus, ZnSe thin films can be used as buffer layer for Cu(In,Ga)(S,Se)2 material, due to its wide direct band gap, high transmittance in blue spectral region with low absorbance and high electrical resistivity properties.[14]

Many efforts are currently directed to a new generation of photodiodes based on wide band-gap compound semiconductors. ZnSe meets this requirement because it has a wide band gap (direct band gap, E_g=2.7 eV) and is capable of emitting light in the blue-green region. ZnSe thin films have been usualy grown by molecular beam epitaxy [15] and chemical vapor deposition [16,17]. On the other hand, several reports on the electrodeposition from aqueous solutions [18,19] as well as from molten salts [20] have been published. However, little study has been reported about the sprayed ZnSe thin films. The high-quality, stoichiometry-controlled p-type ZnSe bulk crystals as well as p-type epitaxial layers have been produced by the temperature difference method under controlled vapor pressure (TDM-CVP) [21]. And also the growth of sufficiently low resistivity n-type epitaxial layers on ZnSe substrates is applicable to realize highperformance ZnSe pn junction directly formed on the high quality p-type ZnSe substrates. Although ZnSe is normally n-type, the as grown electrodeposited films present p-type conductivity as inferred from the photoelectrochemical response [22]. Another interesting feature is that depending on the electrodeposition conditions, the

films present either a gray or red coloration depending on whether they have an excess of Zn or Se, respectively. Zinc selenide is semiconducting material with wide band gap (2.7 eV) at room temperature.
Zinc selenide (ZnSe) thin films were deposited onto glass substrates by the quasi-closed volume technique under vacuum. The film structure was studied by X-ray diffraction (XRD) technique, scanning electron microscopy and atomic force microscopy (AFM). The investigations showed that the films are polycrystalline and have a cubic (zinc blende) structure. Structural investigations show that ZnSe films deposited by the quasi-closed volume technique under vacuum are polycrystalline and have a zinc blende structure. A preferential orientation of film crystallites with (1 1 1) planes parallel to the substrate was observed. In order to obtain samples with stable structure and reproducible properties all films were subjected to a heat treatment. The polycrystalline structure of films plays an important role in the mechanism of electrical conduction. The values of optical bandgap were determined from the absorption spectra.[23]

The process of spray pyrolysis was first introduced in the 1942's for the preparation of transparent oxide films. Since it has become one of the more extensively used low cost and readily scaleable techniques, spray pyrolysis has been reviewed several times in the literature [24,25]. One of its early applications was the deposition of thin films of sulphide by Chamberlin and his co-workers and also the chemical spray process has been used successfully for inorganic films and to deposite a great many compounds of CdS, CdSe, ZnS, ZnSe, CdZnS and Cu_2S by R.R. Chamberlin and J.S. Skarman [26,27]. Subsequently they extended the process to the preparation of thin film $CdS/Cu_{2-x}S$ photovoltaic cells with the achievement of 2% efficiency. The technique was then adopted by the Stanford University group led by Bube, who eventually used the method to deposited a wide range of compound semiconductors. Starting with thin film of CdS, they were able to within a short period prepare solar cells by the spray pyrolysis of CdS films onto a single crystal CdTe substrate and thereby produce devices with 6% efficiency. They then extended the work to the deposition of (Cd,Zn)S films onto p-type single crystal CdTe substrates, thus forming solar cells and achieving efficiencies between 6% and 8% [28-30].

The chemical spray process has been used successfully for inorganic films and to deposite a great many compounds of CdS, CdSe, ZnS, ZnSe, CdZnS and Cu_2S by R.R. Chamberlin and J.S. Skarman They showed that the semiconductor characteristics of a spray deposited film are most dependent on the solution composition, substrate temperature, and the crystallinty of the substrate. Parameters such as spray rate, solution concentration, and the substrate thermal environment are the parameters which are adjusted such that a physically uniform film results. The crystallinity of the spray deposited film is dependent on the substrate and the starting material, particularly the cation material such as cadmium chloride or cadmium acetate in a cadmium thiourea solution [31-33].

Thin films of ZnSe has attracted considerable interest over the years owing to their wide range of applications in various opto-electronic devices and in solar cells [34]. It has a direct band gap (2·67 eV) and transparent over a wide range of visible spectrum. More progress has been achieved in fabrication of blue-green light emitting diodes, dielectric mirrors, filters and other optically sensitive devices [35].

High crystalline quality of ZnSe based layers can be obtained by epitaxial growth on GaAs substrates due to the small lattice mismatch. The growth process has been successfully improved and optimized during recent years, resulting in laser diodes with an emission wavelength in the gren spectral range with a lifetime of a few hundred hours in continuous wave operation [36]. An alternative approach for growing high-quality ZnSe based layers is the use of ZnSe substrates. However, the structural quality of the homoepitaxially grown layers is often poor [37], despite the theoretical advantages of the non-polar interface and the nearly perfect matching of thermal expansion coefficients. The remaining oxide on the substrate surface, which is responsible for the generation of dislocations, has been proposed as one reason for this [38]. In order to remove the oxide and thereby reduce the defect densities, the preparation of the substrates prior to the growth by an in situ hydrogen plasma cleaning process was proposed [39]. By this method layers with a high crystalline quality could be realized

and lasers with an operation lifetime exceeding two hours were obtained by Katayama K et al.[40].

Zinc selenide is n-type semiconducting material with wide band gap (2.7 eV) at room temperature. It is suitable for red, blue and green light emitting diodes [41–44], photovoltaics [43-45], laser screens [46], thin film transistors [47], photoelectrochemical cells [48–50], etc. Nowadays, ZnSe thin films have been used as an n-type window layer for thin film heterojunction solar cells. Also interest in ZnSe–GaAs heterojunction has greatly increased in recent years because of possible applications in a number of high speed and optoelectronic devices [51,52]. The wide band gap ZnSe and related ternary alloys such as Zn1–xCdxSe, ZnSe1–ySy, etc. makes them promising materials for optoelectronic device technology in the blue region of the visible spectrum [53,54].

Thermally evaporated ZnSe thin films deposited on glass substrates within substrate temperatures (Ts) at 303 K–623 K are of polycrystalline nature having f.c.c. zincblende structure. The lattice parameter, grain size, average internal stress, microstrain, dislocation density and degree of preferred orientation in the film are calculated and correlated with Ts.[55]

Thin films of sphalerite-type ZnSe were grown by atomic layer deposition (ALD) from elemental Zn and Se precursors. ZnSe grown by ALD is in consequence a promising material for the fabrication of semiconductor-based white light emitting thin film electroluminescence displays. In this paper, we demonstrate white light emission from thin films of ZnSe layers grown by ALD from a synthesis reaction of zinc and selenium. ZnSe films were grown on either quartz or glass substrates, or on a GaAs (0 0 1) substrate. The latter films are crystalline, whereas films grown on quartz or glass are amorphous and investigated their some important properties by E.Guziewicz and et al.[56].

Thin films show different physical properties from bulk materials. So far a number of theoretical and experimental investigations have been carried out to develop different

types of thin films for various purposes. Different techniques have been used to produce thin films such as moleculer beam epitaxy, screen printing, chemical vapor deposition, evaporation, elecrodeposition, spraying pyrolysis and sputtering techniques. Every process has some distinct advantages and disadvantages in terms of material quality and suitability to device fabrication and cost.

In general, the approach in aqueous solution is to grow the films from a Zn salt and SeO_2 in acid medium with a large [Zn^{+2}] : [SeO_2] ratio, fixing the deposition potential in the interval where the code position is carried out under limiting current control [9]. Another interesting feature is that depending on the sprayed conditions, the films present either a blue or a green coloration depending on whether they have an excess of Zn or Se, respectively.

In this study, Zn:Se volume ratio was changed by 0.2:1, 0.4:1, 0.6:1, 0.8:1, 1:1 for depositing ZnSe thin films by spray pyrolysis method at 430 ^{o}C substrate temperature. The effect of Zn:Se ratio on photoconducting of ZnSe films was studied by optical absorption and transmission, I-V characteristics in dark and under light and rise and decay times . It was observed that the Zn:Se ratio as 0.2:1 gives the best results.

CHAPTER 2

THEORY OF SEMICONDUCTOR

2.1. Semiconductor materials

A semiconductor is a material with an electrical conductivity that is intermediate between that of an insulator and a conductor. A semiconductor behaves as an insulator at very low temperature, and has an appreciable electrical conductivity at room temperature although much lower conductivity than a conductor. Commonly used semiconducting materials are silicon, germanium, and gallium arsenide.

The most commonly used semiconductor material is Silicon. This is an element, it has 14 electrons, and its pure solid form melts at 1420 °C. Used for thousands of years to make ordinary glass, Silicon is a very common element. Silicon turns up in lots of rocks and forms the sand on beaches.The earliest commercial semiconductor devices mostly used Germanium. This element has 32 electrons per atom and melts at 985 °C. It has now largely fallen into disuse because it is much rarer and more expensive than Silicon and has no real advantages for most purposes. The second most common modern material is Gallium Arsenide, GaAs. This is a combination of Gallium, an element with 31 electrons per atom, and Arsenic, with 33 electrons per atom. This is a crystalline compound, *not* an element. Hence we can get an extra degree of control over its properties by varying the relative amount of Gallium and Arsenic. GaAs has the advantage of making semiconductor devices which respond very quickly to electrical signals. This makes it better than Silicon for doing tasks like amplifying the high frequency (1GHz to 10GHz) signals from TV satellites, etc. The main disadvantage of GaAs is that it is more difficult to make and the chemicals involved are quite often poisonous. GaAs can be used with signal frequencies up to about 100 GHz. At even higher frequencies more esoteric materials such as Indium Phosphide (InP) may be used. At present, however, the MMWave region (frequencies above about 50 GHz) is only used for special purposes, so most of the electronics in the world thends to be based on Silicon, with some GaAs, and only a few InP devices.

A semiconductor can be distinguished from a conductor by the fact that, at absolute zero, the uppermost *filled* electron energy band is fully filled in a semiconductor, but only partially filled in a conductor.

The distinction between a semiconductor and an insulator is slightly more arbitrary. A semiconductor has a band gap which is small enough such that its conduction band is *appreciably* thermally populated with electrons at room temperature, whilst an insulator has a band gap which is too wide for there to be appreciable thermal electrons in its conduction band at room temperature.

A relatively small group of elements and compounds has an important electrical property, semi-conduction , in which they are neither good electrical conductors nor good electrical insulators. Instead, their ability to conduct electricity is intermediate. These materials are called semiconductors, and in general, they do not fit into any of the four structural materials categories based on atomic bonding. Metals are inherently good electrical conductors. Ceramics and polymers (non-metals) are generally poor conductors but good insulators. The three semiconducting elements (Si, Ge, and Sn) from column IVA of the periodic table serve as a kind of boundary between metallic and nonmetallic elements. Silicon (Si) and germanium (Ge), widely used elemental semiconductors, are excellent examples of this class of materials. Another important semiconductor material is GaAs, a compound of the group IIIA element Ga; and the group V element, As. [57-58]

Semiconductor devices are small but versatile units that can perform an amazing variety of control functions in electronic equipment. Like other electron devices, they have the ability to control almost instantly the movement of charges of electricity. They are used as rectifiers, detectors, amplifiers, oscillators, electronic switches, mixers, and modulators.

In addition, semiconductor devices have many important advantages over other types of electron devices. They are very small and light in weight (some are less than an inch long and weigh just a fraction of an ounce). They have no filaments or heaters, and therefore require no heating power or warm-up time. They consume very little power.

They are solid in construction, extremely rugged, free from microphonics, and can be made impervious to many severe environmental conditions. The circuits required for their operation are usually simple. [59-60]

Semiconductors are a group of materials having electrical conductivities intermediate between metals and insulators. It is significant that the conductivity of these materials can be varied over wide ranges by changes in temperature, optical excitation, and impurity content. This variability of electrical properties makes the semiconductor materials natural choices for electronic device investigations. Semiconductor materials are found in column IV and neighboring columns of the periodic table as shown in Table 2.1. The column IV semiconductors, silicon and germanium, are called elemental semiconductors because they are composed of single species of atoms. In addition to the elemental materials, compounds of column III and column V atoms, as well as certain combinations from II and VI, make up the intermetallic, or compound, semiconductors. As Table 2.1 indicates, there are numerous semiconductor materials.

(a)	II	III	IV	V	VI
		B	C		
		Al	Si	P	Se
	Zn	Ga	Ge	As	Se
	Cd	In	Sn	Sb	Te
(b)	Elemental	IV compounds	III-V compounds		II-VI compounds
	Si	SiC	AlP		ZnS
	Ge		AlAs		ZnSe
			AlSb		ZnTe
			GaP		CdS
			GaAs		CdSe
			GaSb		CdTe

Table. 2.1 Common semiconductor materials: (a) the portion of the periodic table where semiconductors occur; (b) elemental and compound semiconductors

2.2. Compound II-VI semiconductors

These semiconductors are based on one atomic element from Group II and one atomic element from Group VI, each type being bonded to four nearest neighbors of the other type as shown in Figure 2.1.c. The increased amount of charge from Group VI to Group II atoms tends to cause the bonding to be more ionic than in the case of III-V semiconductors. II-VI semiconductors can be created in ternary and quaternary forms, much like the III-V semiconductors.Although less common than the III-V semiconductors, the II-VI semiconductors have served the needs of several important applications. Representative II-VI semiconductors are ZnS, ZnSe,and ZnTe (which form in the zinc blende lattice structure discussed below); CdS and CdSe, (which can form in either the zinc blende or the wurtzite lattice structure) and CdTe which forms in the wurtzite lattice structure.

Among these, Si is used for the majority of semiconductor devices; rectifiers, transistor. The compounds are used most widely in devices requiring the emission or absorption of light. Fluorescent materials such as those used in television screens usually are II-VI compound semiconductors such as ZnS. Light detectors are commonly made with InSb, CdSe, or other compounds such asd the lead salts PbTe and PbSe; Si and Ge are also widely used as infrared and nuclear radiation detectors. An important microwave device, the Gunn diode, is usually made of GaAs.

2.3. Band theory of solids

A useful way to visualize the difference between conductors, insulators and semiconductors is to plot the available energies for electrons in the materials. Instead of having discrete energies as in the case of free atoms, the available energy states form bands. Crucial to the conduction process is whether or not there are electrons in the conduction band. In insulators the electrons in the valence band are separated by a large gap from the conduction band, in conductors like metals the valence band overlaps the conduction band, and in semiconductors there is a small enough gap between the

valence and conduction bands that thermal or other excitations can bridge the gap. With such a small gap, the presence of a small percentage of a doping material can increase conductivity dramatically.

An important parameter in the band theory is the Fermi level, the top of the available electron energy levels at low temperatures. The position of the Fermi level with the relation to the conduction band is a crucial factor in determining electrical properties.

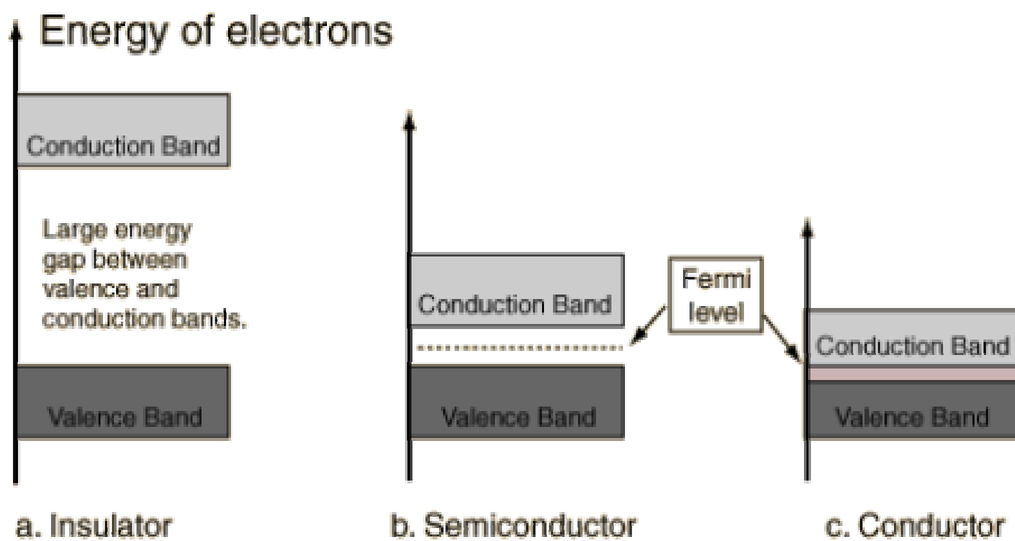

Figure.2.1 Energy Bands for Solids

In solid state physics and related applied fields, the band gap is the energy difference between the top of the valence band and the bottom of the conduction band in insulators and semiconductors. It is often spelled "bandgap".

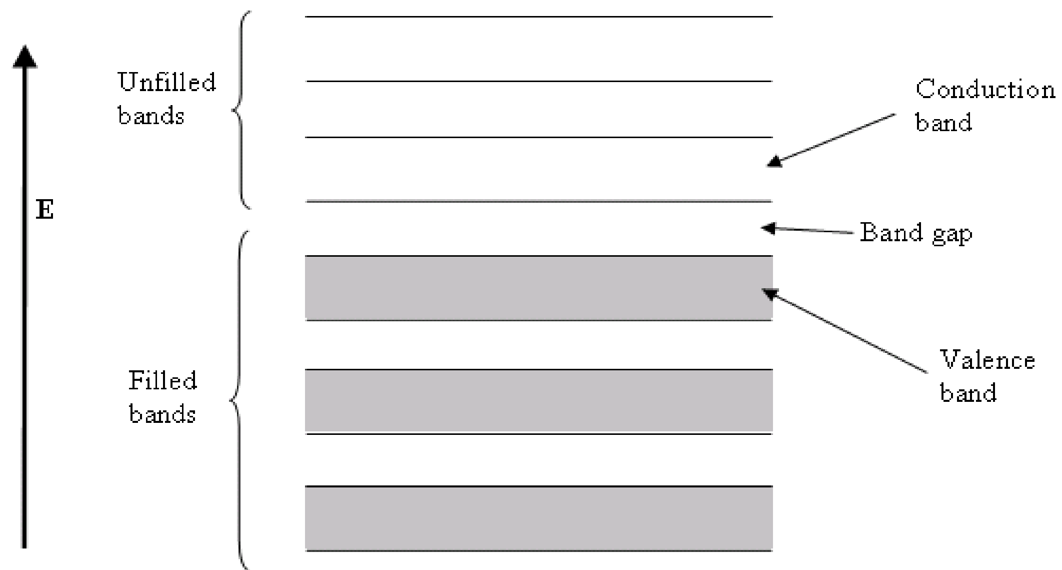

Figure 2.2 A band gap model in insulators and semiconductors

2.4. Semiconductor band structure

An intrinsic (pure) semiconductor's conductivity is strongly dependent on the band gap. The only available carriers for conduction are the electrons which have enough thermal energy to be excited across the band gap, which is defined as the energy level difference between the conduction band and the valence band.

Conductivity is undesirable, and larger band gap materials give better performance. In infrared photodiodes, a small band gap semiconductor is used to allow detection of low-energy photons.

Band gap engineering is the process of controlling or altering the band gap of a material by controlling the composition of certain semiconductor alloys, such as GaAlAs, InGaAs, and InAlAs. It is also possible to construct layered materials with alternating compositions by techniques like molecular beam epitaxy. These methods are exploited in the design of heterojunction bipolar transistors (HBTs) and laser diodes.

Band gap decreases with increasing temperature, in a process related to thermal expansion. Special purpose integrated circuits such as the DS1621 exploit this property

to perform accurate temperature measurements. Band gap also depends on pressure. Bandgaps can be either direct or indirect bandgaps, depending on the band structure.

In semiconductors and insulators, the conduction band is the range of electron energy, higher than that of the valence band, sufficient to make the electrons free to accelerate under the influence of an applied electric field and thus constitute an electric current.

In solids, the valence band is the highest range of electron energies where electrons are normally present at zero temperature. In semiconductors and insulators, there is a bandgap above the valence band, followed by a conduction band above that. In metals, the conduction band is the valence band. The rest of this article refers to the valence band in semiconductors and insulators

Semiconductors and insulators owe their low conductivity to the properties of the valence band in those materials. It just so happens that the number of electrons is precisely equal to the number of states available up to the top of the valence band. There are no available states in the bandgap. This means that when an electric field is applied, the electrons cannot increase their energy (i.e. accelerate) because there are no states available to the electrons where they would be moving faster than they are already going.

There is some conductivity in insulators, however. This is due to thermal excitation - some of the electrons get enough energy to jump the bandgap in one go. Once they are in the conduction band, they can conduct electricity, as can the hole they left behind in the valence band. The hole is an empty state which allows electrons in the valence band some degree of freedom.

It is a common misconception to refer to electrons in insulators as "bound" - as if they were somehow attached to the nucleus and couldn't move. Electrons in insulators are quite free to move - in fact they move at a speed on the order of 100 km (60 mi) per second! They are also delocalised, having no well defined position within the sample.

The distinction between semiconductors and insulators is a matter of convention. One approach is to consider semiconductors a type of insulator with a low band gap. Insulators with a higher band gap, usually greater than 3 eV, are not considered semiconductors and generally do not exhibit semiconductive behaviour under practical conditions. Mobility also plays a role in determining a material's informal classification.

2.5. Doping of semiconductors

One of the main reasons that semiconductors are useful in electronics is that their electronic properties can be greatly altered in a controllable way by adding small amounts of impurities. These impurities are called dopants.

Heavily doping a semiconductor can increase its conductivity by a factor greater than a billion. In modern integrated circuits, for instance, heavily-doped polycrystalline silicon is often used as a replacement for metals.

2.6. Intrinsic and extrinsic semiconductors

An intrinsic semiconductor is a semiconductor which is pure enough that the impurities in it do not appreciably affect its electrical behavior. In this case, all carriers are created by thermally or optically excited electrons from the full valence band into the empty conduction band. Thus equal numbers of electrons and holes are present in an intrinsic semiconductor. Electrons and holes flow in opposite directions in an electric field, though they contribute to current in the same direction since they are oppositely charged. Hole current and electron current are not necessarily equal in an intrinsic semiconductor, however, because electrons and holes have different effective masses (crystalline analogues to free inertial masses).

The concentration of carriers in an intrinsic semiconductor is strongly dependent on the temperature. At low temperatures, the valence band is completely full, making the material an insulator *(see electrical conduction for more information)*. Increasing the temperature leads to an increase in the number of carriers and a corresponding increase in conductivity. This principle is used in thermistors. This behavior contrasts sharply

with that of most metals, which tend to become less conductive at higher temperatures due to increased phonon scattering.

An extrinsic semiconductor is a semiconductor that has been doped with impurities to modify the number and type of free charge carriers present.

A semiconductor which is doped to such high levels that the dopant atoms are an appreciable fraction of the semiconductor atoms is called degenerate. A degenerate semiconductor acts more like a conductor than a semiconductor.

2.6.1. n-type doping

The purpose of n-type doping is to produce an abundance of mobile or "carrier" electrons in the material. To help understand how n-type doping is accomplished, consider the case of silicon (Si). Si atoms have four valence electrons, each of which is covalently bonded with one of four adjacent Si atoms. If an atom with five valence electrons, such as those from group 15 *(a.k.a. group V)* of the periodic table (e.g. phosphorus (P), arsenic (As), or antimony (Sb)), is incorporated into the crystal lattice in place of a Si atom, then that atom will have four covalent bonds and one unbonded electron. This extra electron is only weakly bound to the atom and can easily be excited into the conduction band. At normal temperatures, virtually all such electrons are excited into the conduction band. Since excitation of these electrons does not result in the formation of a hole, the number of electrons in such a material far exceeds the number of holes. In this case the electrons are the *majority carriers* and the holes are the *minority carriers*. Because the five-electron atoms have an extra electron to "donate", they are called donor atoms. Note that each movable electron within the semiconductor is never far from an immobile positive dopant ion, and the n-doped material normally has a net electric charge of zero.

2.6.2. p-type doping

The purpose of p-type doping is to create an abundance of holes. In the case of silicon, a trivalent atom (such as boron) is substituted into the crystal lattice. The result is that one

electron is missing from one of the four covalent bonds normal for the silicon lattice. Thus the dopant atom can accept an electron from a neighboring atoms' covalent bond to complete the fourth bond. Such dopants are called acceptors. The dopant atom accepts an electron, causing the loss of one bond from the neighboring atom and resulting in the formation of a "hole". Each hole is associated with a nearby negative-charged dopant ion, and the semiconductor remains electrically neutral as a whole. However, once each hole has wandered away into the lattice, one proton in the atom at the hole's location will be "exposed" and no longer cancelled by an electron. For this reason a hole behaves as a quantity of positive charge. When a sufficiently large number of acceptor atoms are added, the holes greatly outnumber the thermally-excited electrons. Thus, the holes are the *majority carriers*, while electrons are the *minority carriers* in P-type materials. Blue diamonds (Type IIb), which contain boron (B) impurities, are an example of a naturally occurring P-type semiconductor.

2.7. Direct transition and indirect transition

Bulk semiconductors are characterized by the structure of their conduction and valence bands as being direct or indirect, so are semiconductor nanocrystals. Direct semiconductor nanocrystals (e.g. CdSe, CdS) are characterized by having the minimum transition energy to promote an electron from the valence band to the conduction band without a change in the electron momentum (the energy of this energy separation is known as the band-gap). For indirect semiconductors however excitation at the band gap energy must be accompanied by a change in the electron's momentum (supplied by a phonon).

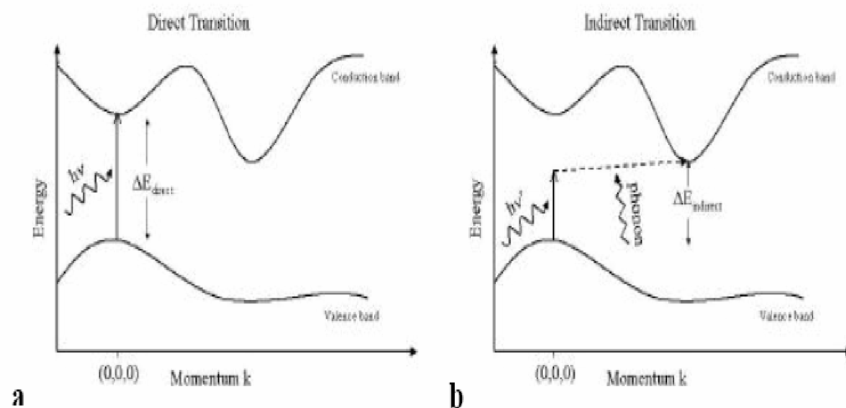

Figure 2.3 (**a**) Direct transition via photon absorbtion. (**b**) Indirect transition via photon *and* phonon absorption (for momentum conservation).

While both types of semiconductors are efficient absorbers of light, it has only been the direct semiconductors which have been emissive enough to be used as an optical source (e.g. in semiconductor GaAs quantum well lasers, in 1991) or as fluorescent labels (CdSe). The discovery of porous silicon as an efficient luminescent material has created great excitement as a prospective candidate for opto-electronic circuit integration. [Integrating direct semiconductor structures on silicon have been unsuccessful due to lattice mismatch]. Though the waited for advances have not materialized, it has been the starting point for experimental and theoretical investigations on nanocrystalline silicon.

2.8. Impurities

Carefully prepared semiconductor materials have a crystal structure. In this type of structure, which is called a lattice, the outer or valence electrons of individual atoms are tightly bound to the electrons of adjacent atoms in electron–pair bonds, as shown in Fig. 2.4. Because such a structure has no loosely held electrons, semiconductor materials are poor conductors under normal conditions. In order to separate the electron pair bonds and provide free electrons for electrical conduction, it would be necessary to apply high temperatures or strong electric fields.

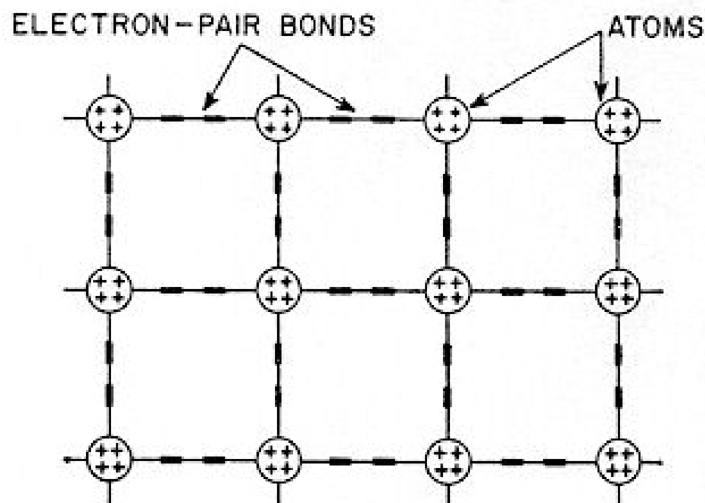

Figure 2.4 Crystal lattice structure.

Another way to alter the lattice structure and thereby obtain free electrons, however, is to add small amounts of other elements having a different atomic structure. By the addition of almost infinitesimal amounts of such other elements, called "impurities", the basic electrical properties of pure semiconductor materials can be modified and controlled. The ratio of impurity to the semiconductor material is usually extremely small, in the order of one part in ten million. (0.1 ppm)

When the impurity elements are added to the semiconductor material, impurity atoms take the place of semiconductor atoms in the lattice structure. If the impurity atoms added have the same number of valence electrons as the atoms of the original semiconductor material, they fit neatly into the lattice, forming the required number of electron–pair bonds with semiconductor atoms. In this case, the electrical properties of the material are essentially unchanged.

When the impurity atom has one more valence electron than the semiconductor atom, however, this extra electron cannot form an electron pair bond because no adjacent valence electron is available. The excess electron is then held very loosely by the atom, as shown in Fig. 2.5, and requires only slight excitation to break away. Consequently,

the presence of such excess electrons makes the material a better conductor, i.e., its resistance to current flow is reduced.

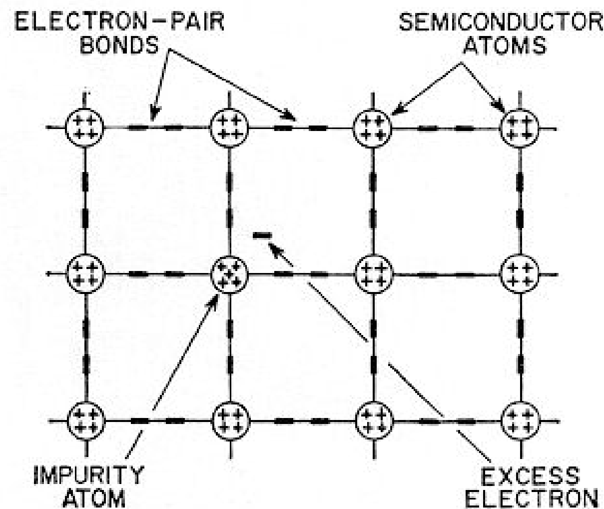

Figure 2.5 Lattice structure of n-type material.

Impurity elements which are added to germanium and silicon crystals to provide excess electrons include arsenic and antimony. When these elements are introduced, the resulting material is called n–type because the excess free electrons have a negative charge. (It should be noted, however, that the negative charge of the electrons is balanced by an equivalent positive charge in the center of the impurity atoms. Therefore, the net electrical charge of the semiconductor material is not changed.)

A different effect is produced when an impurity atom having one less valence electron than the semiconductor atom is substituted in the lattice structure. Although all the valence electrons of the impurity atom form electron–pair bonds with electrons of neighboring semiconductor atoms, one of the bonds in the lattice structure cannot be completed because the impurity atom lacks the final valence electron. As a result, a vacancy or "hole" exists in the lattice, as shown in Fig. 2.6. An electron from an adjacent electron–pair bond may then absorb enough energy to break its bond and move through the lattice to fill the hole. As in the case of excess electrons, the presence of "holes"

encourages the flow of electrons in the semiconductor material; consequently, the conductivity is increased and the resistivity is reduced.

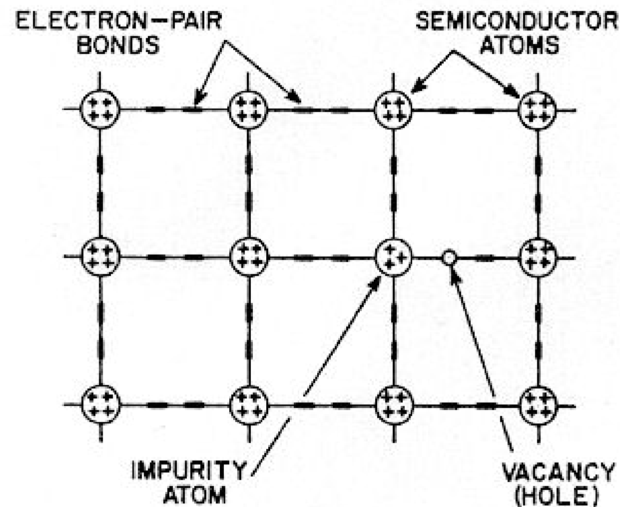

Figure 2.6 Lattice structure of p-type material.

The vacancy or hole in the crystal structure is considered to have a positive electrical charge because it represents the absence of an electron. (Again, however, the net charge of the crystal is unchanged.) Semiconductor material which contains these "holes" or positive charges is called p–type material. p–type materials are formed by the addition of aluminum, gallium, or indium.

Although the difference in the chemical composition of n–type and p–type materials is slight, the differences in the electrical characteristics of the two types are substantial, and are very important in the operation of semiconductor devices**.**

2.9. Absorption of semiconducting materials

2.9.1. Optical absorption

An important tecnique for measuring the band gap energy of a semiconductor is the absorbtion of incident photons by the material. In this experiment, photons selected wavelenght are directed at the sample and the relative transmision of the various photons is observed. Since photons with energies greater than the band gap energy are absorbed while photons with energies less than band gap are transmitted, this experiment gives an accurate measure of the band gap energy.

2.9.2. Transmission and absorption

It is apperent that a photon with energy $h\nu > E_g$ can be absorbed in a semiconductor(Fig.2.7).Since the valence band contains many electrons and the conduction band has many empty states into which the electrons may be excited, the probability of the photon absorption is high.

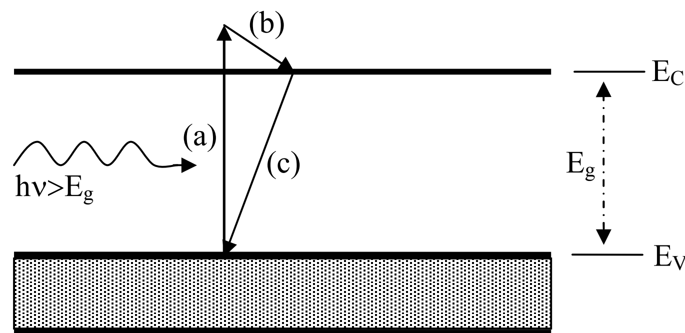

Figure 2.7.Obtical absorbtion of a photon with hv > E_g :(a) an EHP is created during photon absorption; (b) the excited electron gives up energy to the lattice by scatterring events; (c) the electron recombines with a hole in the valence band.

As Fig.2.7 indicates, an electron excited to the conduction band by optical absorption may have more energy than is common for conduction band electrons (almost all electrons are near E_c unless the sample is very heavily doped). Thus the excited electron loses energy to the lattice in scatterring events untill its velocity reaches the thermal equilibrium velocity of other conduction band electrons. The electron and hole created by this absorption process are excess carriers; Since they are out of balance with their

environment, they must eventually recombine. While the excess cariers exist in their respective bads, however they are free to contribute to the coductivity of the material.

A photon with energy less than E_g is unable to excite an electron from the valence band to the conduction band. Thus in a pure semiconductor, there is negligible absorption of photons with $h\gamma < E_g$. One exception to this rule is that a small amount of absorption can occur within a given band (free carrier absorption) ; for example, a low-energy photon can excite a conduction band electron temporarily to a higher state within the conduction band. No excess carriers are created in this process. This component of absorption is usually negligible compared with band-to-band excitation (intrinsic absorption) by photons of higher energy and most photons with $hv < E_g$ are transmitted through the material. This explains why some materials are transparent in certain wavelength ranges.

2.9.3. Absorption constant and band gap

If a beam of photons with $h\gamma > E_g$ falls on a semiconductor, there will be some predictable amount of absorption, determined by the properties of the material. We would expect to ratio of transmitted to incident light intensity to depend on the photon wavelength an the thickness of the sample. To calculate this dependence, let us assume that a photon beam of intensity I_0 (photons/cm^2 –sec) is directed at a sample of thickness I (fig.2.8). The beam contains only photons of wavelength λ, selected by a monochromator. As the monochromator, as the beam passes through the sample, its

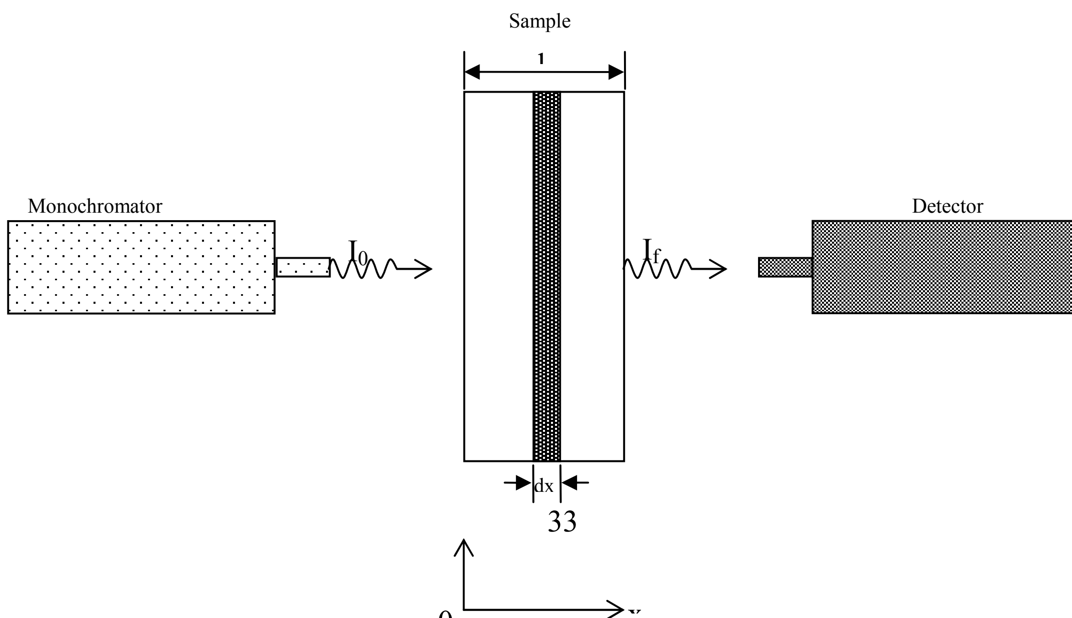

intensity at a distance x from the surface can be calculated by considering the probability of absorption within any increment dx. Since a photon

Figure 2.8. Optical absorption experiment

which has survived to x without absorption has no memory of how far it has travelled, its probability of absorption in any dx is constant [61].

Assume that a semiconductor is illuminated from a light source with hγ greater than E_g and a photon flux of I_0 . As the photon flux travels through the semiconductor, the fraction of the photon absorbed is proportional to the intensity of the flux. Therefore the number of photons absorbed within an incremental distance Δx (Fig.2.9a) is given $\alpha I_0(x)\Delta x$, where "a" is a proportionality constant defined as the absorption coefficient. From continuity of photon flux as shown in fig.2.9a, we obtain

$$I(x+\Delta x)-I(x) = -\alpha I(x)\,\Delta x \qquad (2.1)$$

or

$$\frac{dI(x)}{dx} = -\alpha I(x) \qquad (2.2)$$

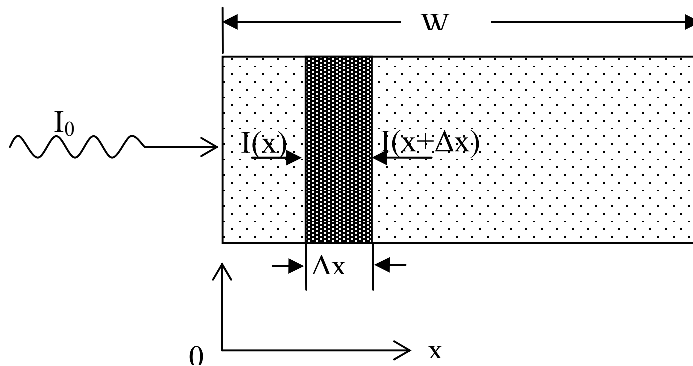

(a)

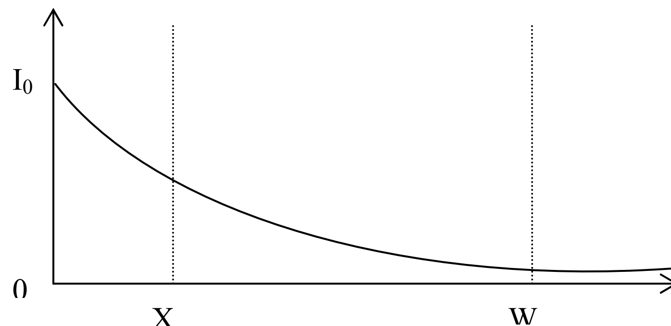

(b)

Figure 2.9 Optical absorption (a) Semiconductor under illumination (b) Exponential decay of photon flux.

The negative sign indicates decreasing intensity of the photon flux due to absorption. The solution of Eq.2.2 with the boundary condition I (0) = I_0 at x=0 is

$$I(x)=I_0\, e^{-\alpha x} \qquad (2.3)$$

The fraction of photon flux that exists from the other and of the semiconductor at x=I (Fig.2.9.b) is

$$I(I) = I_0\, e^{-\alpha I} \qquad (2.4)$$

As an alternative to a transmission experiment, it is possible to monitor the resistance of the sample and observe the photon energy at which absorption takes place .Since absorbed photons create EHP's and these carriers are able to participate in conduction, the conductivity of the sample will increase when photons are absorbed. This change in the conductivity with optical absorption called photoconductivity.

Fig 2.10 indicates the band gap energies of some of the common semiconductors relative

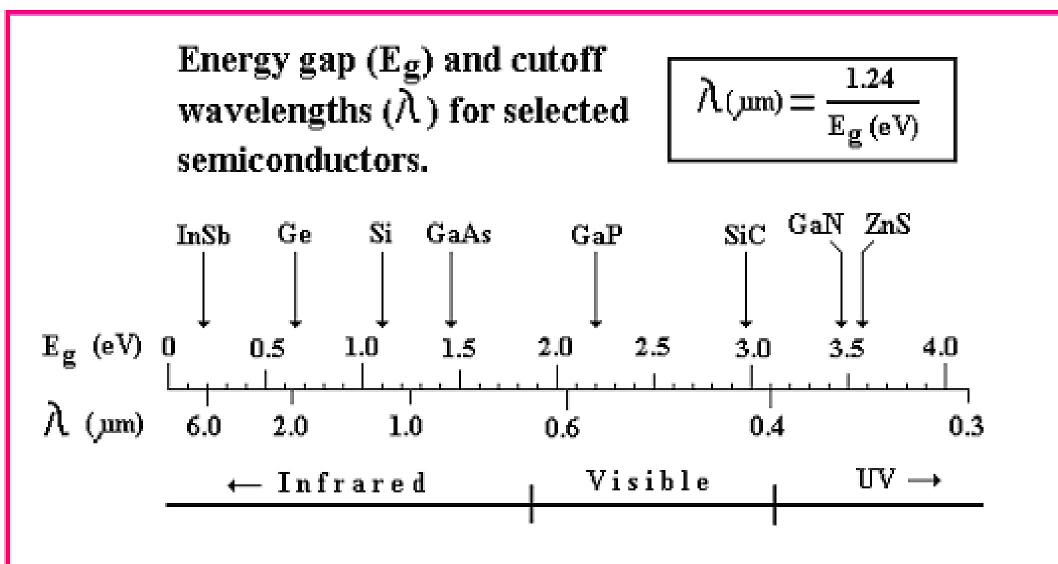

to the visible infrared and ultraviolet portions of the spectrum.
Figure 2.10.Band gaps of some common semiconductors relative to the optical spectrum.

We observe that GaAs, Si, Ge, and InSb lie outside the visible region so that if the eye is to be used as detector in the transmission experiment, an infrared converter tube must be used. Other semiconductors, such as GaP and CdS , have band gaps wide enough to pass photons in the visible range. It is important to note here that a semiconductor absorbs photons with energies equal to the band gap, or larger [61].

2.10. Hall mobility

The importance of the Hall effect is underscored by the need to determine accurately carrier density, electrical resistivity, and the mobility of carriers in semiconductors. The Hall effect provides a relatively simple method for doing this. Because of its simplicity, low cost, and fast turn around time, it is an indispensable characterization technique in the semiconductor industry and in research laboratories. In a recent industrial survey, it is listed as one of the most-commonly used characterization tools. Furthermore, two recent Nobel prizes (1985, 1998) are based upon the Hall effect. The history of the Hall effect begins in 1879 when Edwin H. Hall discovered that a small transverse voltage appeared across a current-carrying thin metal strip in an applied magnetic field. Until that time, electrical measurements provided only the carrier density-mobility product, and the separation of these two important physical quantities had to rely on other difficult measurements. The discovery of the Hall effect removed this difficulty. Development of the technique has since led to a mature and practical tool, which today is used routinely for testing the electrical properties and quality of almost all of the semiconductor materials used by industry.

It is possible to determine drift mobility by generating electrons (and holes) by exposure to light. The electrons are drift down a length of the material under the influence of a field of known strength and their arrival at some point detected by a collector. If the light

is attenuated by a shutter, the time between the light exposure and arrival of the electrons at the collector can be used to determine the drift mobility.

In practice, it is usually more convenient to determine mobility termed the Hall mobility. For silicon and germanium, these two mobilities are approximately equal. If a charge moves in a magnetic field, than it experiences a force acting at right angles to both its direction and the direction of the magnetic field. This is well-known left-hand rule or motor rule for the exerted by a magnetic field on a conductor carrying a current. If the thumb and first and second fingers of the left hand are made mutually perpendicular and if the forefinger indicates direction of the magnetic field and the second finger the direction of the current than the thumb indicates the direction of the resultant force. Since the conventional current flow is from high to low potential this is also the direction of movement of positive charges.

If we now consider the carriers in the semiconductors, they will move under the influence of an electric field: Electrons against the field, holes with the field. If we apply a magnetic field at right angels to the electric field, in addition; I vector will be introduced instead of the travelling straight toward the ends of the bars, the electrons or holes will also move in a direction mutually perpendicular to the two fields. They will take paths shown by in Fig.2.11. Both holes and electrons will move transversely in the some direction since although

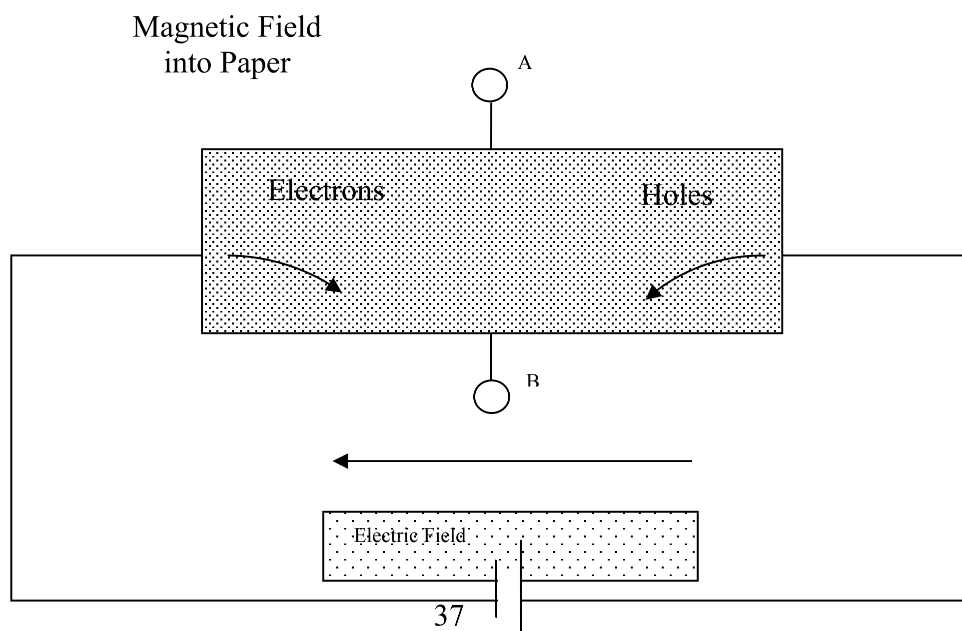

Figure 2.11 Hall Effect

the action of the magnetic field is reversed, the motions laterally are in opposite directions. A space charge builds up at the lower surface and at equilibrium an electric field is setup across the crystal such that is magnitude and direction balance the space charge and charge flow straight through the crystal. If we connect a potentiometer across the field, i.e., at A and B, the polarity will indicate whether holes or electrons are the majority carrier and magnitude of the potential difference will indicate the hall field induced.

As might be expected the force exerted on the charge is proportional to the magnetic field and to the electric field and the velocity of the charge. In fact these last two are related, the stronger the field the higher velocity for any particular crystal and these is the relationship used to define mobility.

$$\mu_n = \frac{V_D}{E} \qquad (2.5)$$

If we consider the condition necessary for charge to move undeflected through the crystal, than the Hall field E_H must exactly compensate the force exerted by the magnetic field, for any charge carrier

$$eE_H = eV_DH \qquad (2.6)$$

where e is the charge on electron, V_D velocity of charge carrier, and H is the magnetic field, or E_H can be obtained from the above equation as,

$$E_H = V_DH \qquad (2.7)$$

The Hall voltage will depend on the Hall field and distance across it,

$$V_H = E_H d \tag{2.8}$$

By combining these various equations, it can be seen that Hall mobility

$$\mu_H = \frac{V_H}{E_H d} \tag{2.9}$$

or , since

$$\mathbf{E} = \frac{V}{I} \tag{2.10}$$

where V_a is the applied voltage and I is length of bar,

$$\mu_H = \frac{V_H I}{V_a H d} \tag{2.11}$$

Since all the parameters on the right can be measured, hall mobility can be calculated [62].

CHAPTER 3

EXPERIMENTAL STUDIES

THIN FILM PRODUCTION TECHNIQUES

3.1. Spray pyrolysis method

3.1.1. Introducion

The spray pyrolysis technique (or solution spraying) for the growth of semiconducting films is a method of spraying a suitable solution mixture onto a heated substrate. It is a convenient and economical method for the deposition of such mareials.This technique is simply consist of spraying a finely atomised solution onto a suitable hot substrate. The substrate temperature has a greate influence on the spraying of the thin films. The spray nozzle which is used for strongly affects the spraying rate, the sprayed particle size and the spray distribution.. In the spray pyrolysis process the uniformity of the droplet size is one of the primary requirments for a spray system. The chemicals contained in the spray solution are expected to fulfill the following conditions;

(i)- The chemicals in solution the spraying provide species/complexes that will undergo a thermally activeted chemical reaction to yield the desired thin film material,

(ii)- the remainder of the constituents including the carrier liquid should be volatile at the substrate temperature [63].

3.1.2. Experimental set-up of spraying system:

In this study, the apparatus which is used for the development of thin film samples based on the spraying pyrolysis technique has been designed and developed in our laboratory. A schematic block diagram of an experimental apparatus used for spray pyrolysis is shown in figure 3.1. This system consist of a spraying system, heater, temperature control system, and timer. The system is enclosed by a glass chamber.

3.1.3. Deposition apparatus

In this thesis, the apparatus which we used for the development of the thin film samples based on the spraying pyrolysis technique. This apparatus whose schematic diagram is given in Fig.3.1 consists of a spraying system, heater, temperature control system and timer.

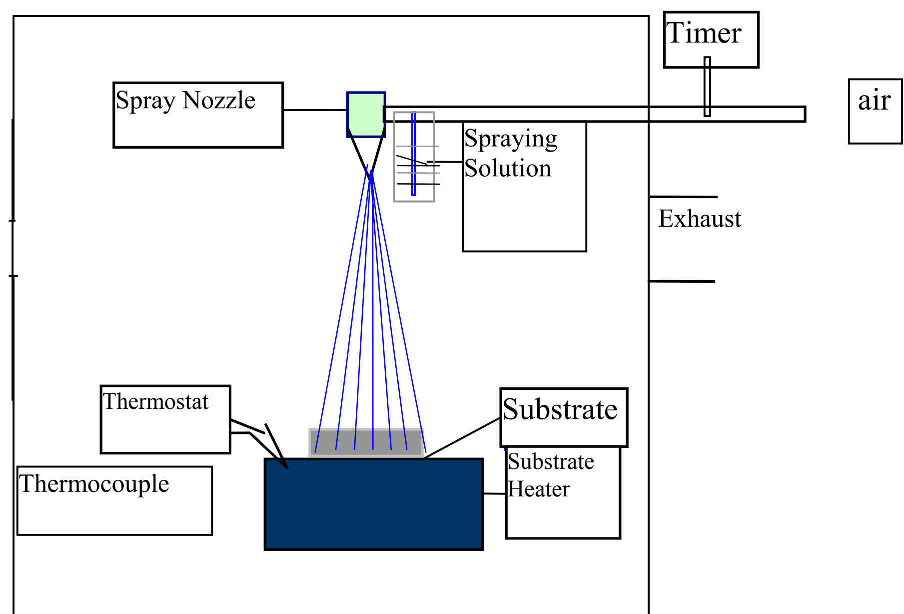

Figure 3.1. Schematic diagram of the spray pyrolysis system.

Spraying system: This is used to produce the bubbles from the spraying solution. The bubbles can be in different sizes depending on the geometry of the nozzle, as seen in Fig.3.1 above, being employed to produce the bubbles and also the flow rate of the

carrier gas. In this study, air is used as carrier gas and the flow rate of the spraying solution is regulated by air.

Heater: This is used to heat the substrates. It is consisted of a steel plate with a resistance coil lying under it . The power of the heater is 2500 watts and it operates at 220 volts and 50 Hz (AC).

Temperature control system : A thermostat is used to keep the substrates at required temperatures. One of the most important factors which plays a vital role for producing high quality thin film samples is to keep the substrates at required temperatures. The substrate temperature is controlled to within an accuracy of $\pm 5^{0}C$ by thermostat system.

Glass chamber: The spraying system and the heater are placed in a glass chamber and nitrogen gas is passed through during the growth of the thin film.

3.2 Growth mechanism of the semiconducting thin films by the spraying pyrolysis method

3.2.1 Introduction

The spray pyrolysis technique for the production of semiconducting films is a method of spraying suitable solution mixtures onto a heated substrate. This method is convenient and economical method for the deposition of such materials. Several factors influence the proper peformance and the quality of semiconducting thin film produced by the spraying pyrolysis method. These factors are as follows: (i) the properties of substrate, (ii) the substrate temperature, (iii) the spray nozzle, (iv) the uniformity of the droplet size of solution, (v) the flow rate of spraying solution, (vi) the height of the nozzle from the substrate surface.

3.2.2. Substrate preparation

The physical properties of substrates on which thin films is deposited, play a vital role in the growth of good quality thin film samlpes. The film properties are very strongly dependent on the crystal structure of substrate. The crystalline films can be deposited on a noncrystalline material such as glass, ceramic and mica. For example, a highly crystalline film from the zinc cloride ($ZnCI_2$) solutions can be developed on an amorphous substrate. In this study, glass is used as substrate because of its cheepless when compared to other types of substrate. The preparation of glass substrate is as follows. Firstly, the glass substrates are cut into 0.5 cm^2 in size. A cleaning process of the glass substrate is carried out in four steps as seen in Fig.3.2

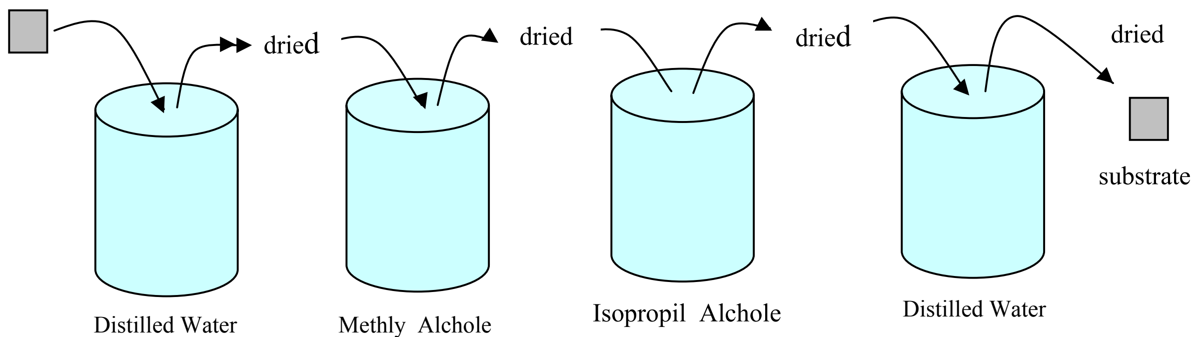

Figure.3.2 Cleaning process of the glass substrate.

The cleaning process is as follows:

1- The glass substrate is immersed into the distilled water to clean the dust on its surface for 15 minutes. Then it is taken out from the distilled water and dried.
2- The substrate which is taken from the the first cup and dried, is immersed into the methyl alcohol and left there for 15 minutes to clean the oil substance on the surface of the substrate, and then it is taken out from this liquid and dried in air.
3- The dried substrate is immersed into the third cup filled with isopropil alcohol and it is treated again for 15 minutes to obtain a smooth surface.
4- Finally, the substrate is treated with the distilled water as in the first step to clean all the residues remaining on the surface of substrate during the other processes.

3.2.3 Spraying solution preparation

The spraying solution is prepared for the production of ZnSe thin film as follow; firstly, the required amounts of $ZnCI_2$ and SeO_2 salts are weighed by high sensible electronic balance and stirred together into a cup containing the distilled water of 100 mlt to form the solution. Different spraying solutions were used for the production of semiconducting ZnSe thin films with different compositions.

3.2.4 Development of ZnSe thin films

To develop polycrystalline ZnSe thin film samples, a 100 mlt spraying solution of $ZnCI_2$ and SeO_2 with different ratios were used. The ZnSe thin films were prepared by spraying an aqueous solution of $ZnCl_2$ and SeO_2 on glass substrate kept at 430 ^{o}C. The atomization of the chemical solution into a spray of fine droplets is effected by the spray nozzle, with the help of compressed air as carrier gas. By varying the volume of $ZnCl_2$ solution, Zn:Se ratio was varied as 1:1, 0.8:1, 0.6:1, 0.4:1, 0.2:1 and thin films prepared. During the spraying process the substrates were heated by an electrical heater. The substrate temperature was measured using an iron-constantan thermocouple. The solution flow rate was kept at 5 $cm^3 min^{-1}$ and the height of the nozzle was fixed to 20 cm from the substrate placed on the heater. Then the spraying solutions were sprayed onto the glass substrate which was kept at 430^{0}C temperature. When the solution droplets reach to the heated glass substrate surface, the following chemical reaction occurs,

$$ZnCl_2 + SeO_2 + H_2O \longrightarrow ZnSe + 2HCI + (3/2)O_2 \quad (3.1)$$

As seen from this reaction, a ZnSe thin film is formed on the glass substrate surface. All spraying processes were carried out in air.

CHAPTER 4
RESULTS AND DISCUSSIONS

4.1 The Thickness determination Of Znse thin films

The thicknesses of the samples were obtained by using the weighing method. This method is explained by the following expression:

$$t = \frac{(m_2 - m_1)}{\rho A} \qquad (4\text{-}1)$$

where ρ is the density of the ZnSe thin films (ρ= 5.4 gr/cm^3), m_1 is the weight of the glass substrate before the film growht and m_2 is the weight of the same glass substrate after the ZnSe samlpe growth on it, and A is the area of the glass substrate. As seen from Table 1, the thickness of the ZnSe thin films were determined between 0.9 and 1.6 μm .

4.2. Optical studies

An important technique used for the determination of the band gap energy of a semiconductor is the absorption of incident photons by material. Optical absorption studies of the sprayed ZnSe thin films on the glass substrate have been carried out in the wavelength range of 300 nm to 900nm employing a UV/VIS spectrophotometer (Jasco 7800 model). To determine the energy band gap values of the samples, it is necessary to determine the value of the absorption coefficients of the samples corresponding to different wavelengths of the photons. For this purpose, a Jasco 7800 Model Spectrometer was used for the transmission and absorption measurements. The absorption coefficient of sample corresponding to different wavelengths can be calculated from following equation:

$$\frac{I}{I_0}(transmission) = e^{-\alpha t} \qquad (4\text{-}2)$$

where t is the thickness of the thin film sample, T=I/I_0 is transmittence. (I_0 is incident light intensity and I is transmitted light intensity)

By using α values, the optical band gap of the thin film sample can be determined by means of the following equation:

$$\alpha = \frac{A}{h\nu}(h\nu - E_g)^{1/2} \qquad (4\text{-}3)$$

where A is a constant, E_g energy band gap of thin film, h is Planck constant, $\nu=c/\lambda$, c is light speed and λ is wavelenght of light. A similar curve like in Fig.4.4 can be obtained plotting the linear extrapolation of $(\alpha h\nu)^2$ versus $h\nu$ for thin film sample. The band gap of the sample is evaluated from this curve drawing a tangent line to the curve as seen in following Fig.4.4, where $h\nu$ is the photon energy, E_g denotes the optical energy bandgap, and A the characteristic parameter (independent of photon energy) for respective transitions. Fig.4.9 shows that the dependences of $(\alpha h\nu)^2$ as a function of photon energy $h\nu$ indicates the direct nature of band-to-band transitions for the studied samples. The values of optical bandgap, E_g have been determined by extrapolating the lineer portions of respective curves to $(\alpha h\nu)^2 \rightarrow 0$.

4.3. The crystal structure Of the thin film samples

4.3.1. X-ray diffraction study

Structural properties of the deposited thin films were studied by X-ray diffraction (XRD) technique. The X-ray measurements were performed using CuKα radiation (λ=1.542Å) from a conventional θ - 2θ diffractometer (D 5000 Siemens). The peaks (2θ) of the XRD patterns of the thin film samples were identified by using Bragg diffraction law equation as given follows.

The lattice constant 'a' for the cubic phase structure is determined by the relation

$$a^2 = \frac{\lambda^2(h^2 + k^2 + l^2)}{4\sin^2\theta} \qquad (4\text{-}4)$$

where θ is the diffraction spectra (Bragg's angle), λ is the wavelength of the x-ray. The line profiles were measured by means of point by point cutting using a fix period 20s and 2θ increment of 0.02^o.

4.4. Electrical measurements

In this study, the Van der Pauw method will be used to measure the resistivity, conductivity and Hall coefficient of the thin film samples. To apply this method, four indium ohmic contacts A,B,C and D are prepared on the semiconducting samples by the evaporation method as seen in figure 4.1

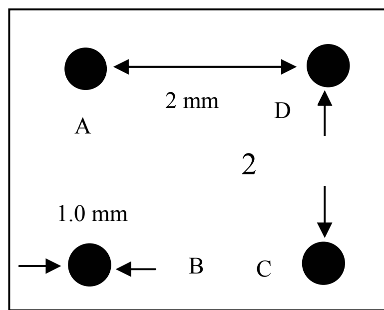

Figure 4.1 In-ohmic contacts prepared on thin film samples.

4.4.1. Resistivity and conductivity measurements

The resistivity measurement was carried out in two steps establishing an experimental set-up as seen in figure 4.2

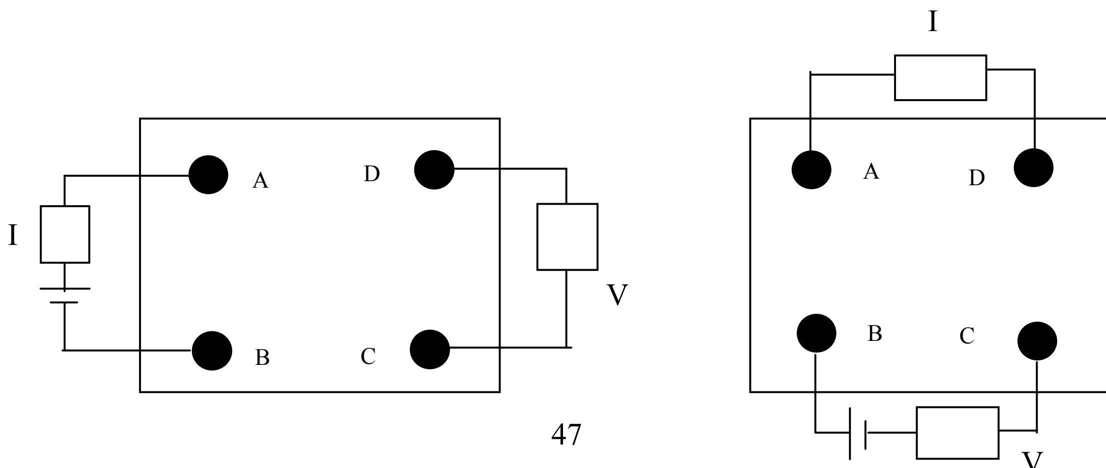

(a) (b)

Figure 4.2 Resistivity measurement set-up

Applying an input potential V_{in} across the contacts A and B, current I_{AB} is obtained. On the other hand, a potential V_{CD} appears between the contacts C and D. $R_{AB,CD}$ denotes the ratio of voltage V_{CD} measured between contacts C and D, to the current I_{AB} following between A and B. To determine the resistance $R_{BC,DA}$ at this time, the input potential is applied across the contacts B and C. Then, the current I_{BC} flows across the contacts B and C and the potential V_{DA} is measured between these contacts.

The resistivity of sample is calculated by using the following equation :

$$\rho = \left(\frac{t}{\ln 2}\right)(R_{AB,CD} + R_{BC,DA})F\left(\frac{R_{AB,CD}}{R_{BC,DA}}\right) \tag{4-5}$$

where t is the thickness of the thin film and F is a function. If $R_{AB,CD}$ and $R_{BC,DA}$ are nearly equal to each other, the approximate value of F can be obtained from following expression:

$$F = 1 - \left(\frac{R_{AB,CD} - R_{BC,DA}}{R_{AB,CD} + R_{BC,DA}}\right)^2 \left(\frac{\ln 2}{2}\right) - \left(\frac{R_{AB,CD} - R_{BC,DA}}{R_{AB,CD} + R_{BC,DA}}\right)^4 \left(\frac{(\ln 2)^2}{4} - \frac{(\ln 2)^3}{12}\right) \tag{4-6}$$

4.4.2. Hall mobility measurements

Thin film sample is placed in a magnetic field perpendicular to the sample plane and the $R_{AC,DB}$ resistance value is measured for a few times and the average value of the $R_{AC,DB}$ is taken. The experimental set up for the Hall Mobility measurement is seen in following figure 4.3

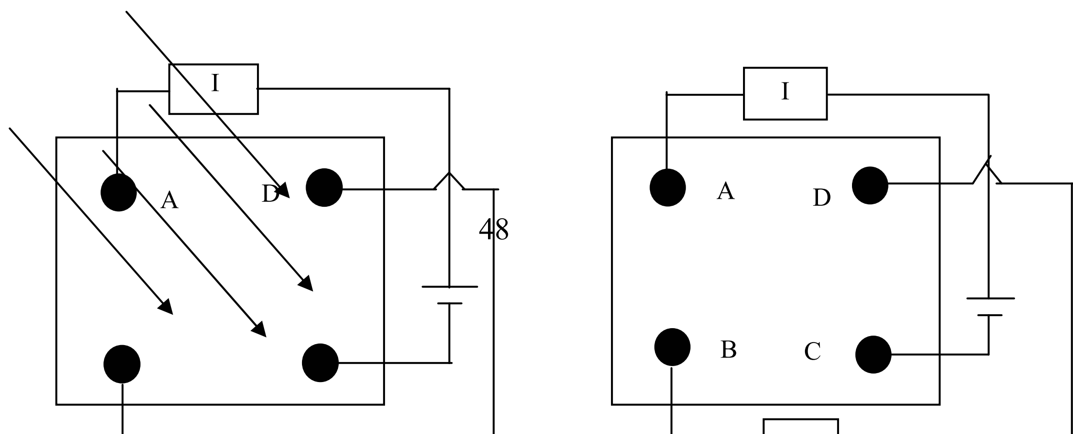

(a)

Figure 4.3 The standart configuration used for hall effect measurement

The Hall Mobility can be calculated substituting the measured values of $R_{AC,DB}$, the applied magnetic field, B, and thickness of the thin film layer, t,in the following expression;

$$\mu = \left(\frac{t}{B}\right)\left(\frac{R_{AC,DB}}{\rho}\right) \qquad (4\text{-}7)$$

where t is the thickness and ρ is the resistivity of the thin film.

4.5. Results and discussion

4.5.1. The thickness determination of ZnSe thin films

The thicknesses of the samples were obtained by using the weighing method. This method was explained by Equ.4.1. The thickness measurement results are given in following table.

Sample number	Zn:Se ratio	Thickness of the thin films (μm)
1	0.2:1	0.64
2	0.4:1	0.97
3	0.6:1	1.29
4	0.8:1	1.10
5	1:1	0.71

Table 4.1 The thickness of ZnSe thin film samples.

4.5.2. Optical Studies

For the determination of the electronic band-edge structure of the thin film samples (sprayed ZnSe), the best method is to study the absorption gap through the measurement of transmission spectra. For this process, we need to spray the samples onto an optically transparent substrate. Therefore, all of the thin films were sprayed onto the glass substrate which is transparent in a spectral region that includes the visible wavelengths. The bandgap of the resulting films were estimated from the transmission spectra using the extrapolation of $(\alpha h\nu)^2$ versus hν. The value of the absorption coefficient (α) was obtained from the value of the transmission by using the Eq.4.3. Optical absorption studies of the sprayed ZnSe thin films on the glass substrate have been carried out in the wavelength range of 300 nm to 900 nm employing a UV/VIS spectrophotometer. The bandgap energy graphs of the ZnSe thin films are given in figures. (Fig.4.4; 4.5; 4.6; 4.7; 4.8)

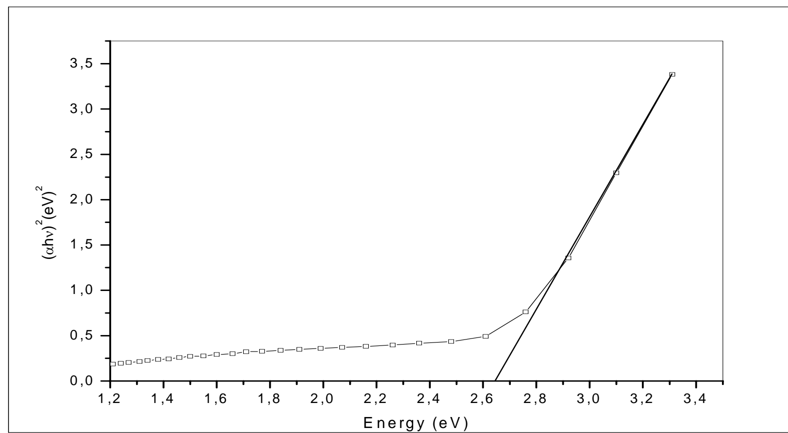

Figure 4.4. Plot of $(\alpha h\nu)^2$ versus photon energy (hν) for film the Zn:Se (0,2:1) thin film grown by using spraying pyrolysis method

As seen from Figure 4.4, the direct band gap material Zn:Se (0,2:1) is capable of emitting light in the red region of the visible spectrum with a wavelength about 470 nm and the average band gap energy values for ZnSe were obtained 2,64 eV. This means that the threshold energies for the photon absorption by ZnSe semiconducting thin films at room temperature is about 2,64 eV.

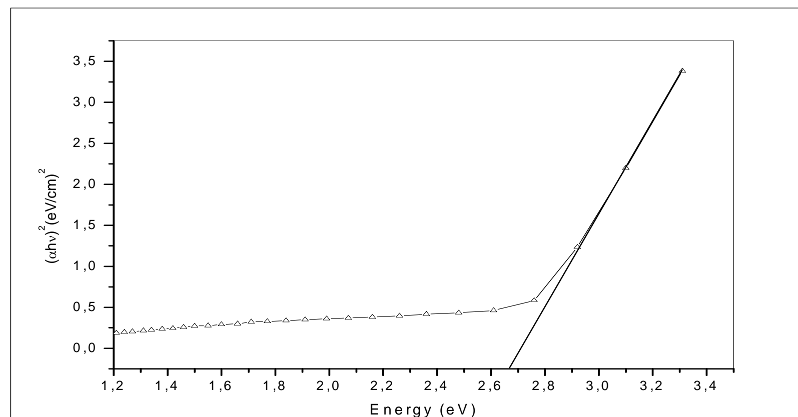

Figure 4.5 Plot of $(\alpha h\nu)^2$ versus photon energy ($h\nu$) for film the Zn:Se (0,4:1) thin film grown by using spraying pyrolysis method

As seen from Figure 4.5 the direct band gap material ZnSe is capable of emitting light in the red region of the visible spectrum with a wavelength about 464 nm and shows the average band gap energy values for ZnSe were obtained 2,67 eV. This means that the threshold energies for the photon absorption by ZnSe semiconducting thin films at room temperature is about 2,67 eV.

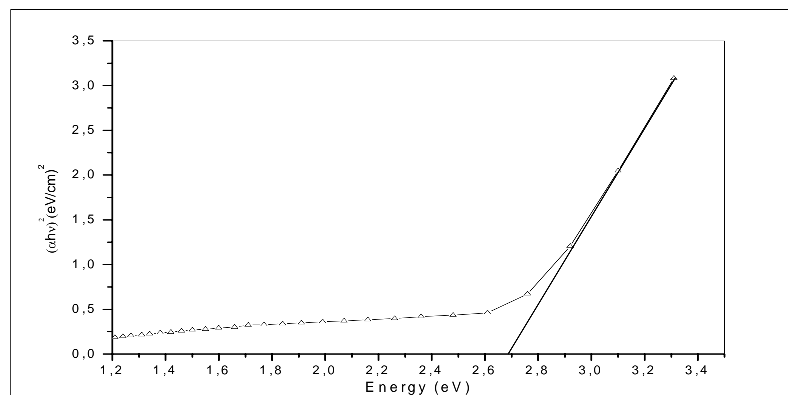

Figure 4.6

Plot of $(\alpha h\nu)^2$ versus photon energy (hν) for film the Zn:Se (0,6:1) thin film grown by using spraying pyrolysis method

As seen from Figure 4.6 the direct band gap material ZnSe is capable of emitting light in the red region of the visible spectrum with a wavelength about 460 nm and shows the average band gap energy values for ZnSe were obtained 2,69 eV. This means that the threshold energies for the photon absorption by ZnSe semiconducting thin films at room temperature is about 2,69 eV.

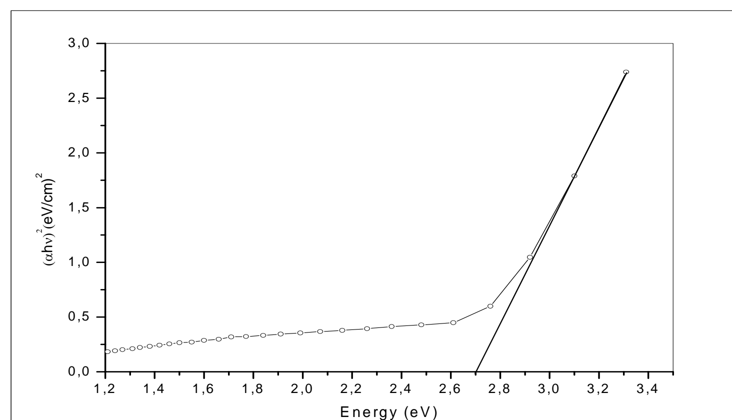

Figure 4.7 Plot of $(\alpha h\nu)^2$ versus photon energy (hν) for film the Zn:Se (0,8:1) thin film grown by using spraying pyrolysis method.

As seen from Figure 4.7 the direct band gap material ZnSe is capable of emitting light in the red region of the visible spectrum with a wavelength about 460 nm and shows the average band gap energy values for ZnSe were obtained 2,70 eV. This means that the threshold energies for the photon absorption by ZnSe semiconducting thin films at room temperature is about 2,70 eV.

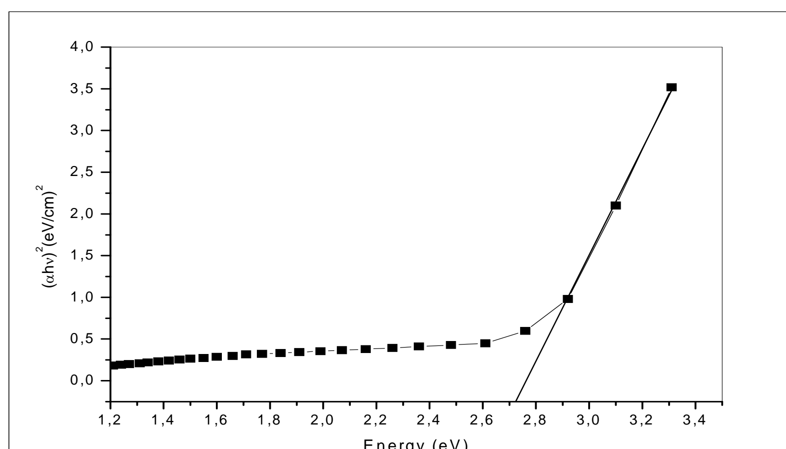

Figure 4.8 Plot of $(\alpha h\nu)^2$ versus photon

energy (hν) for film the Zn:Se (1:1) thin film grown by using spraying pyrolysis method

As seen from Figure 4.8 the direct band gap material ZnSe is capable of emitting light in the red region of the visible spectrum with a wavelength about 457 nm and shows the average band gap energy values for ZnSe were obtained 2,71 eV. This means that the threshold energies for the photon absorption by ZnSe semiconducting thin films at room temperature is about 2,71 eV.

It is seen from Table4.2 and figures (Fig.4.4; 4.5; 4.6; 4.7; 4.8) that the bandgap energy increased from 2.64 eV to 2.71 eV as the Zn ratio was increased from 0.2 :1 to 1:1.

Sample number	Zn:Se ratio	Band gap of the thin films 'E_g' (eV)
1	0.2:1	2.64
2	0.4:1	2.67
3	0.6:1	2.69
4	0.8:1	2.70
5	1:1	2.71

Table 4.2 The band gap energy values of ZnSe thin films

From Figure 4.9, the plots of $(\alpha h\nu)^2$ versus hν indicate that there is some tailing in the band gap below the absorption edge. This indicates that there is a high concentration of impurity states in the thin fims which can cause a perturbation of the band structure with the result that the parabolic distribution of the states will be disturbed by a prolonged tail into the energy gap. Therefore, it is observed that the average transmission in the visible

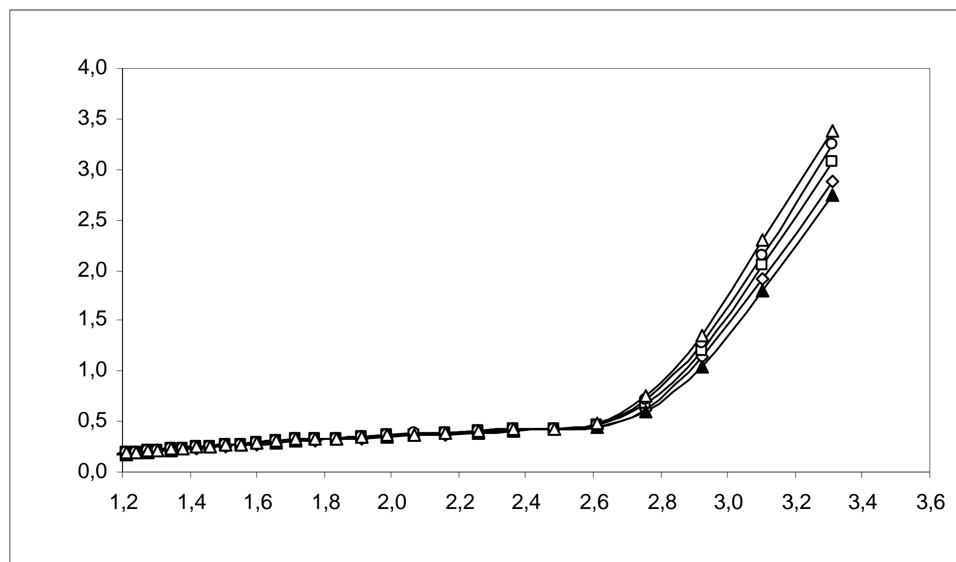

region exceeds 85%. The optical transmittance is slightly improved in the visible range. With increasing the Zn ratio, the optical transmittance decreases not only with the oxidation of zinc, but also as the number of defects (vacancies and interstitial impurities) in the crystalline structure of ZnSe decreases. And the optical properties of the thin films are improved with decreased the Zn ratio, and due to the shift in the transmittance fringes in the samples. The defect density inside the ZnSe thin films gradually decreased with the decrease of the Zn ratio, and the crystalline of the samples is also improved. Thus, with decreasing Zn ratio can increase the homogeneity and crystallinity of the structure of the ZnSe thin films and decrease the defect density at the edge of energy band-gap. Concerning the effect of the Zn ratio, the optical absorption edge shifts to higher wavelengths with decreasing the Zn ratio is observed. It is indicating a decrease of optical band gap from about 2.71 to 2.64 eV. This could be explained by desorption of some extra selenium around grain boundaries, which was already proved by the increase associated to the carrier concentration and hall mobility [64].

Figure 4.9 Plot of $(\alpha h\nu)^2$ versus photon energy ($h\nu$) for film the ZnSe thin films grown by using spraying pyrolysis method

Figure 4.10 shows the relationship of the optical energy band gap with the variation of the Zn ratio. The optical band gap of ZnSe thin films increased with the increase of the Zn ratio, the minimum optical band gap of ZnSe thin films reached to 2.64 eV at the Zn ratio 0.2:1. The maximum optical band gap of the ZnSe thin films is 2.71 eV, that indicates the thermal effect of the metal induced the electrons supply capability of the Zn

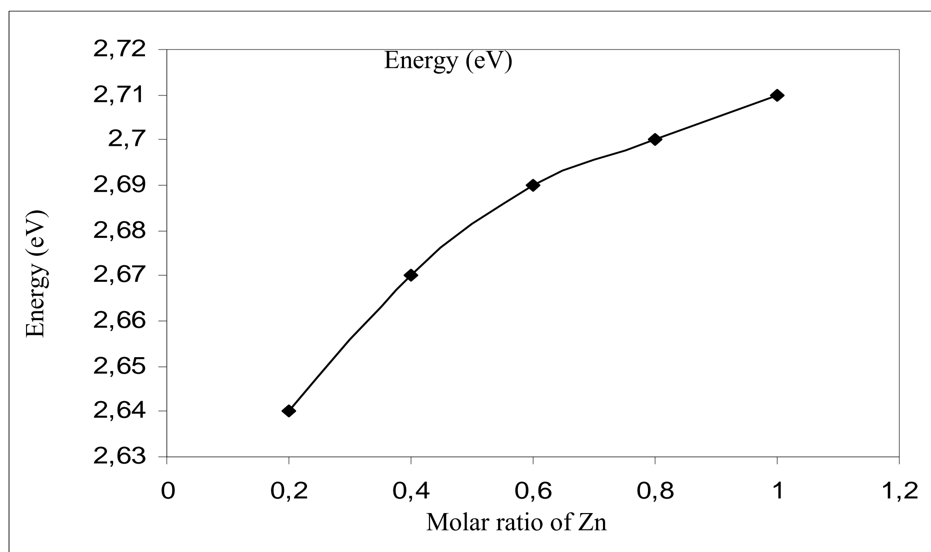

ratio and further improves the compensation effect. In addition, the decreasing of E_g with the Zn ratio can be attributed in terms of inducing crystallization in semiconductor films. This leads to introducing freedom resulting in an increase in capacity of the system. Crystallization via nucleation and growth becomes possible and depends the Zn ratio. Thus, the crystallization of the ZnSe thin films increases with the decreasing the Zn ratio

Figure 4.10 Variation of the bandgap energy versus molar ratio of Zn.

4.5.3. X-ray diffraction

The XRD patterns of sprayed ZnSe thin films prepared at different ratio and constant substrate temperatures are shown in Figure 4.11. The diffractograms indicating the presence of all the promient peaks of ZnSe are arising from (200) reflections from the ZnSe thin films which are polycrystalline, having f.c.c cubic zinc blende structure. It is also observed that the XRD patterns of all ZnSe thin films show a preferred orientation along the (200) plane. The (200) direction is the close-packing direction of the zinc blende structure. As the Zn ratio decreases the peak intensities increase up to , indicating the formation of more crystallites with well-defined orientation (200). Beyond 430^0C, partial decomposition may be taking place, giving rise to a decrease in intensity. And it is important to mention also that when the Zn ratio decreases the relative intensity of the peaks is maintained and their full width at half maximum (FHWM) decreases. The fact that the FHWM decreases is indicative of the improvement of the crystalline quality. It is noticed that the intensities of the phases were enhanced with decreasing the Zn ratio, which may be due to the sufficient increase in the thermal energy for recrystallization and the grain growth with the Zn ratio.

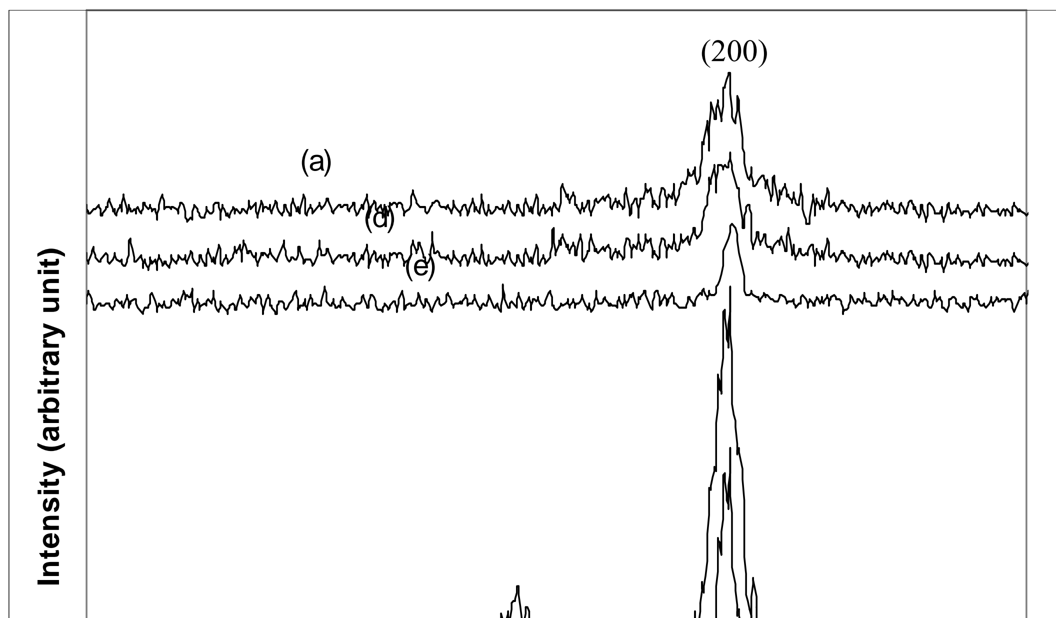

Figure 4.11 X-ray diffraction patterns for different Zn:Se ratios: (a) 1:1; (b) 0.2:1; (c) 0.4:1; (d) 0.6:1; and (e) 0.8:1.

4.5.4. Grain size studies

It is observed that the XRD patterns of all ZnSe thin films show a most preferred orientation along (200) plane. The grain size of the ZnSe thin films were estimated for the (200) plane by using the Scherrer formula [19].

$$d = \frac{\lambda}{D\cos\theta} \qquad (4\text{-}8)$$

where d is the grain size, λ is the x-ray wavelength used, D is the angular line width of the half-maximum intensity and θ is the Bragg angle.

Sample number	Zn:Se ratio	Grain size(A)
1	0.2:1	32
2	0.4:1	29
3	0.6:1	23
4	0.8:1	23
5	1.0:1	22

Table 4.3 Grain size values of the ZnSe thin films with different Zn ratio.

The variation of the grain sizes with Zn:Se ratio is shown in Table.4.3. The grain size 'd' shows a decreasing tendency with Zn ratio increasing at 430^0C substrate temperature. The density of the film is therefore expected to change in accordance with the change of lattice constant and grain size [20,21]. The change in lattice constant for the deposited thin film over the bulk clearly suggests that the film grains are strained which again may be due to the nature and concentration of the native imperfections changing [64].

Figure 4.12 The molar ratio of Zn versus the grain size

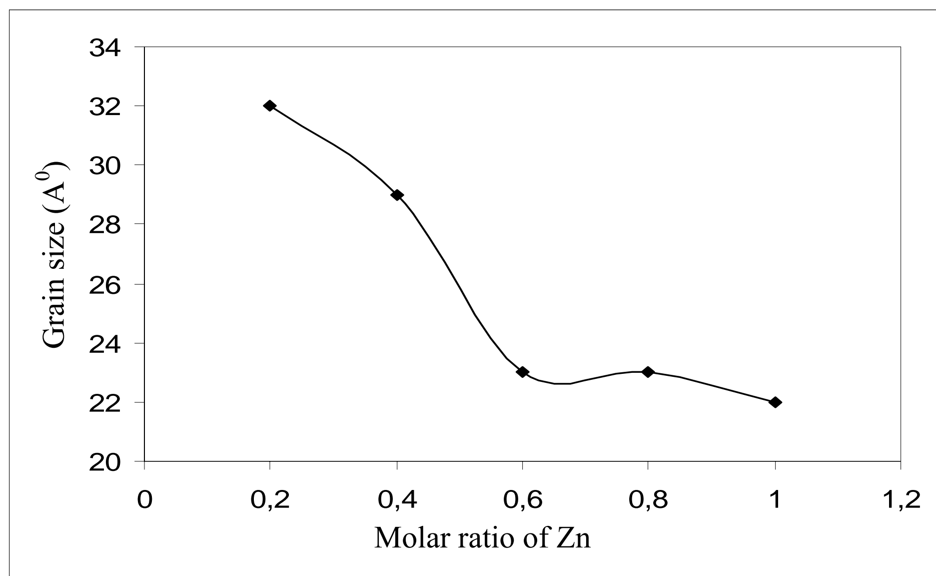

The grain size of the deposited ZnSe thin films is small and within the range $22A^0$ to $32A^0$. The change of grain size with Zn ratio is prominent. From the Figure 4.12, it can be seen that the grain size increases with the decrease of the Zn ratio, which can be understood by considering the merging process induced from the Zn ratio. For ZnSe thin films, there are many dangling bands related to the zinc of selenium defects at the grain boundaries. As a result, these defects are favorable to the merging process to form larger ZnSe grains while decreasing the Zn ratio.

4.5.5. Studies on electrical parameters

The electrical resistivity, conductivity and Hall Mobility of the sprayed ZnSe thin films were measured by using Van der Pauw method at room temperature. The various electrical parameters (resistivity, conductivity and hall mobility) for spray deposited

ZnSe thin films deposited at different Zn ratios are represented in table . The resistivity, conductivity and hall mobility curves against the different Zn ratio of ZnSe thin films are shown in Figure 4.13, 4.14 and 4.15, respectively. The electrical resistivity of the thin film samples vary from 0.86×10^{6} ohm-cm to 1.1×10^{6} ohm-cm, the conductivity of the thin film samples vary from 0.9×10^{-6} $(\text{ohm-cm})^{-1}$ to 1.16×10^{-6} $(\text{ohm-cm})^{-1}$, and the Hall mobility of the thin film samples from 0.47 $cm^2/Vsec$ to 0.61 $cm^2/Vsec$, as the Zn ratio vary from 0.2 to 1 in the ZnSe thin film samples.

The resistivity and conductivity values were calculated from Equ.4.5 and the Hall Mobility values of the thin film samples were calculated from Equ.4.7 and all the calculated values are given in Table 4.4.

Sample number	Zn:Se ratio	Resistivity (10^6) (Ωcm)	Conductivity (10^{-6}) $(\Omega cm)^{-1}$	Hall mobility (cm^2/Vm)
1	0.2:1	0.86	1.16	0.61
2	0.4:1	0.89	1.12	0.54
3	0.6:1	0.93	1.07	0.51
4	0.8:1	0.99	1.01	0.49
5	1:1	1.1	0.9	0.47

Table 4.4 The resistivity, conductivity and Hall Mobility values of ZnSe thin film samples

As seen in Table 4.4, electrical properties of ZnSe semiconducting thin films which have been developed with the different ratio of Zn (Zn:Se=1:1-0.2:1-0.4:1-0.6:1-0.8:1) at substrate temperatures 430^0C are given. In Figure 4.13, 4,14 and 4,15 show the resistivity, conductivity and Hall Mobility curves against the Zn molar ratio. As seen from these curves the resistivity of the ZnSe thin film samples has a maximum value at about Zn molar ratio of 1:1 but the Hall Mobility has a minimum value at the same ratio of the Zn.

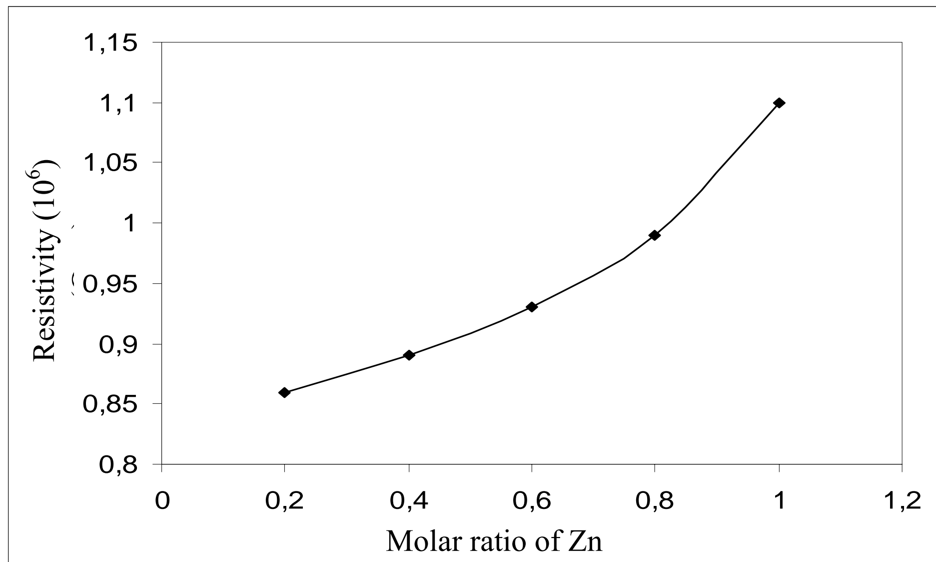

Figure 4.13 The molar ratio of Zn versus resistivity

It can be shown from these results that, if the ZnSe thin film samples are prepared at 1:1 Zn molar ratio they may have a high resistivity and low Hall Mobility. When they are prepared at 0.2 Zn molar ratio, ZnSe thin film samples show a low resistivity ($0.8x10^5$ ohm-cm) and high Hall Mobility (0.61 cm^2/V-sec). It is seen that the Zn ratio decreases, the n-type conduction of the films is confirmed and enhanced. It indicates that a high degree of crystallization is achived the decreasing resistivity due to the reduction in the scattering of the carriers at the grain boundaries and crystal defects, which increaes the Hall Mobility as a consequence of the crystallite size. And the resistivity decreased due to the increase in crystallization and orientation of the crystal structure of the films because the Hall Mobility is increase with the alignment of the orientation of the crystals.In addition to the effect of orientation, the increase in grain-packing density

could also contribute to the decrease in resistivity. Also, excess zinc atoms segregate at the grain boundaries and cause the resistivity of the films to increase. Selenium atoms do not segregate at the boundaries, but they act as a trap for the carriers together with zinc atoms increasing the potential barrier at the grain boundaries leading to an additional increase in the resistivity [65].

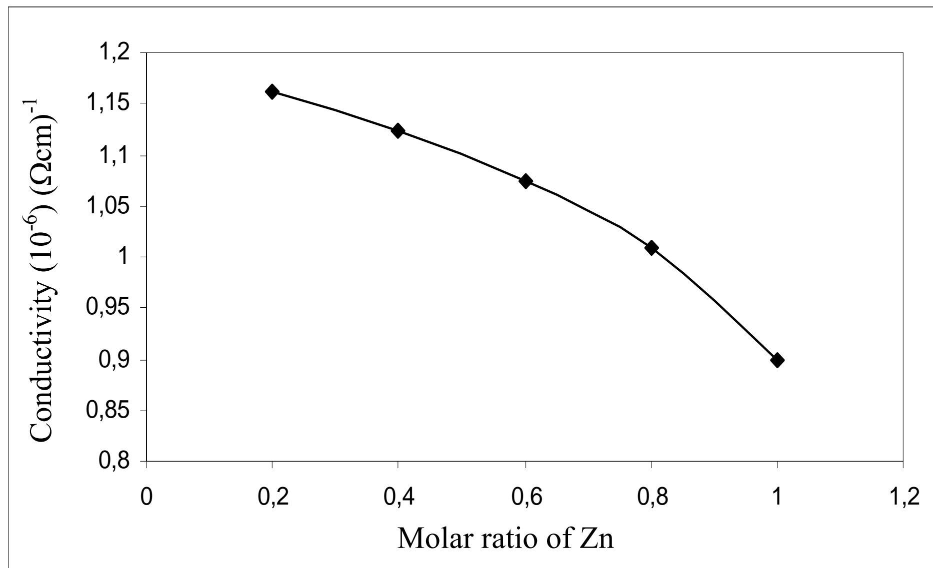

Figure 4.14 The molar ratio of Zn versus the conductivity

And the excess zinc increase the inter-grain barrier heights are increased. When the inter-grain barrier heights increase, the resistivity of the films increases while Hall Mobility decreases as seen in the Figure 4.14.

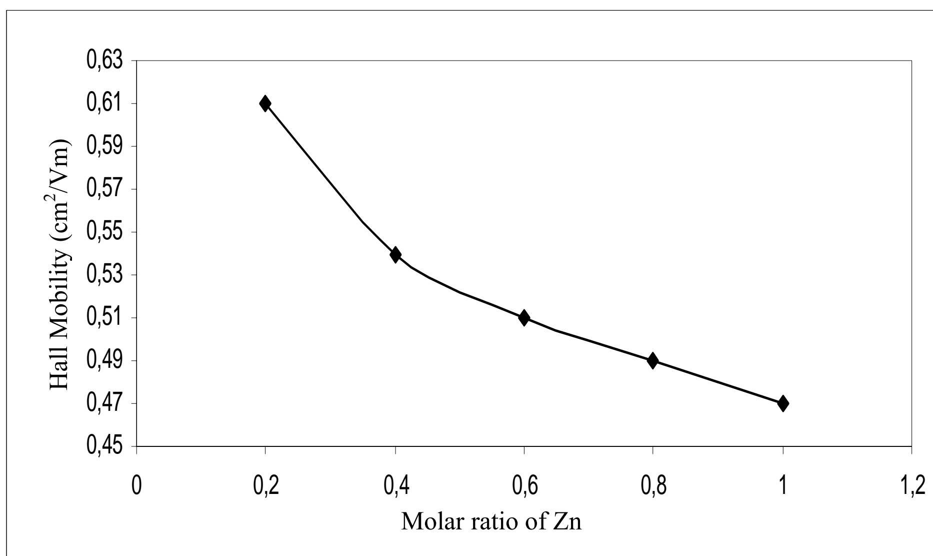

Figure 4.15 The molar ratio of Zn versus the Hall Mobility.

Hence, it can be said that excess selenium acts as a factor that decrease the resistivity of the films while increasing the Hall Mobility. As the Zn ratio decreases for crystallization of ZnSe film leads to the homoganization and stabilization of the crystalline structure of the film.

Electrical measurements here shown that the conductivity, resistivity and Hall Mobility of the sprayed ZnSe thin films are very sensitive to adsorbed oxygen (since chemisorbed oxygen acts as an acceptor impurity). It is well known that oxygen impurity is found as a background impurity in many materials because of its easily diffusing properties into crystal lattice during the production of the films in air. The oxygen impurities are first physically adsorbed at the grain boundaries and on the surface of the ZnSe thin films. Thus, the electrical properties of polycrystalline thin films are limited by the potential barriers created by the grain boundaries. The introduction of oxygen in the thin films can strongly modify the properties of the grain boundaries, then induce on decrease of the electrical conductivity of the films. Moreover, it is observed that the substitution of selenium by oxygen in the ZnSe crystalline matrix also induces an increase of the resistivity of the thin films. The high increase of the electrical resistivity of the films studied can be due both to the grains or their boundaries when oxygen is introduced in the films. The films all have an n-type conductivity, which shows that the introduction of oxygen in ZnSe does not change the type of the majority carriers. As a result, the presence of oxygen impurities aids in recrystallization of the ZnSe films during production process. Therefore, the oxygen impurity can alter the microstructure and the grain size of the sprayed ZnSe films during production process [65].

4.5.6. Conclussion

In this work, semiconducting ZnSe thin films were fabricated under different Zn:Se ratio and constant substrate temperature on the glass substrate by using spraying plyrolsis

method and their growth conditions, crystal structure, optical and electrical properties were investigated in detail using different techniques.

In the spraying pyrolysis method, the thin film quality is strongly dependent on the substrate, the substrate temperature, the distance between the nozzle and substrate and the flow rate of the chemical solution. It was found that the high quality sprayed semiconducting ZnSe thin films could be obtained on a glass substrate at 430^0C substrate temperature and the corresponding flow rates of 0.5 ml, 0.5ml and 0.3.ml per min, respectively. The distance between nozzle and substrate in all the processes was adjusted to be 20 cm.

The optical properties of the semiconducting ZnSe thin films were calculated from optical measurement data. The band gaps ZnSe thin film samples were found as 2.64 eV- 2.71 eV. The crystal structures of the ZnSe semiconducting thin films were investigated by x-ray powder diffractometer and their main diffraction peaks are found to be in agreement with other studies [21, 28, 64, 65]. The diffractograms indicating the presence of all the promient peaks of ZnSe are arising from (200) reflections from the ZnSe thin films which are polycrystalline, having f.c.c cubic zinc blende structure. It is also observed that the XRD patterns of all ZnSe thin films show a preferred orientation along the (200) plane.

The electrical properties of sprayed ZnSe thin films were investigted by using Van der Pauw method. It can be shown from the electrical measuements that, if the ZnSe thin film samples are prepared at 1:1 Zn molar ratio they may have a high resistivity and low Hall Mobility. When they are prepared at 0.2 Zn molar ratio, ZnSe thin film samples show a low resistivity ($0.8x10^5$ ohm-cm) and high Hall Mobility (0.61 cm^2/V-sec).

In this study, all semiconducting sprayed thin films were developed under the influence of the atmospheric conditions, therefore, the quality of the thin films samples are affected from the oxygen absorption during the deposition process. The main effect of oxygen absorption on the samples is a reduction of the Hall mobility and an increase of

the resistivity. Oxygen molecules are known to be first physically adsorbed onto the ZnSe thin film surface and transition from physical to chemical adsorption then takes place by capture of conduction band electrons [39]. Therefore, chemisorption effects on the mobility are attributed to the chemisorption of oxygen at the grain boundaries, which alters the barrier height and barrier width. Because of the small grain boundry area compared to the film surface, however, the charge in electron density should be attributed to the chemisorption of oxygen at the film surface. And also it is shown that the resistivity and the Hall mobility of the samples are strongly dependent on the Zn:Se ratio.

In recent years, sprayed semiconducting thin films have been investigated intensively, in part because of its low cost industrial importance in the microelectronic, solar cells, detectors, light emitting devices industry. Hence, it is our recommendation that a new study should be under taken to determine the optimum conditions on the film growth of the ZnSe and other II-VI compound thin films by changing some growth parameters and substrate.

REFERENCES

[1] V. Kumar, T.P.Sharma, Optical Mat.**10**, (1998) 253.

[2] G. Riveros, H. Gomez, R.Henriguez, R. Schrebler, R.E. Maratti, E.A. Dalchiele., Solar Energy Mat. And Solar Cells, **70**, (2001) 255.

[3] L.Ting Chu and S.C.Shirley, Solid-State Elec.,V.38, No:3, (1995) 533-549.

[4] S.A. Empedocles, D.J. Norris, M.G. Bawendi, Pyhs. Rev. Lett.**77**, (1996) 3873.

[5] C.C. Kim, S.Sivananthan, Phys. Rev. B, **53**, (1996) 1475.

[6] V.L.Colvin, M.C.Schlamp, A.P.Alivisatos, Nature, **370**, (1994) 354

[7] Pradip.KR Kalita, B.K.Sarma and H.L.Das. Bull. Mater. Sci.Vol.23,No.4, (2000) 313-317.

[8] A. Schmidth et al., J.Crystal Growth, **101**, (1990) 758.

9. S.Y. Wang, et al, Applied Phys. Lett., **61**, (1992) 506.

[10] H.Goto, T. Ido, A. Takatsuka, J.of Crystal Growth, **529**, (2000) 214-215.

[11] C.D. Lukhande, P.S. Patil, A. Ennaoui, H. Tributsch, Appl. Surface Sci., **294**, (1998) 123-124.

[12] J.P. Rai, Solar Energy Mat., **30**, (1993) 376.

[13] A. Lizzo, M.A. Tagliente, L. Caneve, S.Scaglione, Thin Solid Films, **8**, (2000) 368.

[14] Materials Research Bulletin 39(2004)1829–1839R.B. Kalea, C.D. Lokhandeb,* and et al.

[15] H.Goto, T.Ido, A.Takatsuka, (2000), J.of Crys.Growth, **529**,214-215.

[16] S.Fujita, Y.Matsuda, A.Sasaki, ,(1984), J.Crys.Growth, **231**,140.

[17] C.D.Lukhande, P.S.Patil, A.Ennaoui, H.Tributsch, Appl.Surface Sci., (1998), **294**,123-124.

[18] J.P.Rai, Sol.Ener.Mat., (1993),**30**,376.

[19] K.Singh, R.K.Pathak, (1994),Electrochem.Acta., **39**, 2683.

[20] S.Sanchez, C.Lucas, G.S.Picard, M.R.Bermejo, Y.Castrillejo, (2000), Thin Solid Films, **107**,361-362

[21] F. Sakurai, M. Motozawa, K. Suto, J. Nishizawa, J. Crystal Growth 172 (1997) 75.

[22] A.P.Samantilleke,M.H.Boyle,J.Young, I.M.Dharmadasa, J.Mater.Sci. 9 (1998) 289.

[23] G.I. Rusu*, M.E. Popa, G.G. Rusu, Iulia Salaoru., Applied Surface Science 218 (2003) 222–230.

[24] K.L.Chopra. (1969). Thin Film Phenomena. *McGraw-Hill Book Company*. Newyork

[25] J.E.Hill, R.R.Chamberlin. (1964*). US Patent*. **3**. 148084

[26] R.R.Chamberlin, J.S.Skarman.(1966). Chemical Spraying Deposition Process for Inorganic Films. *J.Electrochemical Society***.** **113**. 86-90

[27] R.R.Chamberlin, J.S.Skarman. (1966). *Solid State Electronic*. **9**. 819-822

[28] R.S.Feigelson, A.N.Diage, S.Yin, R.H.Bube. (1977). II-VI Solid-Solution Films by Spraying Pyrolysis. *J.Appl.Phys*. **48**. 3162-3165.

[29] Y.Y.Shaiw, A.L.Fahrenbruch, R.H.Bube. (1978). Photovoltaic Properties of ZnCdS/CdTe Heterojunctions Prepared by Spray Pyrolysis. *J.Appl.Phys*. **52**. 4963-4966

[30] T.A.Chynoweth, R.H. Bube. (1980). Electrical Transport in ZnCdS Films Deposited by Spray Pyrolysis. *J.Appl.Phys*. **51**. 1844 –1846

[31] M.Krunks, E.Mellikov, E.Sork. (1986). Formation of CdS Films by Spray Pyrolysis. *Thin Solid Films*. **105**. 145-147

[32] K.L.Chopra, R.C.Kaintla, P.K.Pandya, A.P.Thakoor. (1982). *Physics of Thin Films*. **12**.167-171

[33] K.L.Chopra, S.R.Das*, Thin Film Solar Cells*. (1983*). Plenum Press*. Newyork.

[34] Siche D and Hatmann H 1996 J. Mater. Sci. 31 6171

[35] Schmidt A et al 1990 J. Crystal Growth 101 758

[36] Kato E, Noguchi H, Nagai M, Okuyama H, Kijima S and Ishibashi A 1998 Electron. Lett. 34 282

[37] Heinke H, Behringer M, Wenisch H, Großmann V and Hommel D 1998 J. Cryst. Growth 184/185 587–90

[38] Nakanishi F, Yamada T, Nishine S and Shirakawa T 1996 Proc. Int. Symp. Blue Laser and Light Emitting Diyotes (Chiba, Japan) 340

[39] Jeon M H, Calhoun L C and Park R M 1995 J. Electron. Mater. 24 177

[40] Katayama K et al 1998 Appl. Phys. Lett. 73 102
[41] O. Akira, S. Noriyoshi, S. Zembutsu, J. Appl. Phys. 64 (1988) 654.
[42] Nishhizawa, Junichi, Okunu, Yasuo, Jpn. Annu. Rev. Electron Comput. Telecom. 19 (1986) 325.
[43] H.S. Akber, A.J. Abdulkadier, M.S. Bani, J. Sol. Energy Res. 6 (1988) 49.R.B. Kale, C.D. Lokhande / Materials Research Bulletin 3
[44] C. Falcony, S. Sinencio, J.S. Helmen, J. Appl. Phys. 56 (1984) 1752.
[45] A. Ennaoui, S. Siebntritt, M.C. Lux-Steiner, W. Riedl, F. Karg, Sol. Energy Mater. Sol. cells 67 (2001) 31.
[46] M.P. Kulapov, G.A. Murovick, V.N. Ulasyuk, lzv Akad Nauk SSSR Neorg. Mat. 19 (1983) 1807.
[47] R.R. Alfano, O.Z. Wang, J. Jumbo, B. Bhargava, J. Phys. Rev. (A) 35 (1987) 459.
[48] A.M. Chaparro, M.T. Gutierrez, J. Herrero, J. Klaer, Mater. Res. Soc. Symp. Proc. 668 (2001) H2.9.1.
[49] A. Ennaoui, S. Siebentritt, M.Ch. Lux-Steiner, W. Riedl, F. Karg, Sol. Energy Mater. Sol. Cells 67 (2001) 172.
[50] A. Rumberg, C. Sommerhalter, M. Toplak, A. Jager-Waldau, M.C. Lux-Steiner, Thin Solid Films 361 (2001) 172.
[51] F. Engelhardt, L. Bornemann, M. Kontges, T. Meyer, J. Parisi, E. Pschorr-Schoberrer, B. Hahn, W. Gerhardt, W. Riedl, F. Karg, U. Rau, in: Proceedings of the Second World Conference and Exhibition on Photovoltaic Solar Energy Conversion, 1996, p. 1153.
[52] C.D. Lokhande, P.S. Patil, H. Tributsch, A. Ennaoui, Sol. Energy Mater. Sol. Cells 55 (1998) 379.
[53] H. Luo, J.K. Furdyna, Semicond. Sci. Technol. 10 (1995) 1041.
[54] A. Boney, Z. Yu, W.H. Rowland, W.C. Harsh, J. Vac. Sci. Rep. 14 (1996) 2259.
[55] Pradıp Kr Kalıta*, B K Sarma And H L Das.,Bull. Mater. Sci., Vol. 23, No. 4, August 2000, pp. 313–317.
[56] E.Guziewicz , M.Godlewski , K.Kopalko and et al.,Thin Solid Films 446 (2004) 172–177.

[57] W.R.Runyan, Semiconductor measurements and instrumentation, McGraw-Hill book company, New York 1975.

[58] V.Stupelman and G.Figaretov, Semiconductor Device, Mir.Publishers Mossow, 1976.

[59] P.Bhattacharya, Semiconductor Optoelectronic Device, Prentice Hall Int. Inc., 1994

[60] I.P.Jacques, Optical Process In Semiconductor, Prentice-Hall, Inc. New Jersey, 1971.

[61] S.M.Size, Physics of semiconductor devices, Murray Hill, New Jersey, a division of John wiley&son, 1969

[62] T.E. Jenkins, Semiconductor Science growth and characterization techniques, prentice hall, 1995

[63] K.L.Chopra, S.R.Das, Thin Film Solar Cells, Plenum Press, Newyork.(1983)

[64] M.Bedir, M.Öztaş, Ö.F.Bakkaloğlu,and R.Ormancı, Eur. Phys.J.B 45 (2005) 465-471

[65] M.Öztaş, M.Bedir, Ö.F.Bakkaloğlu, and R.Ormancı, Acta Physica Polonica A (107)3 (2005) 525-534

PUBLICATIONS

1.M. Bedir, M. Öztaş, Ö. F. Bakkaloğlu and R. Ormancı., "*Investigation on structural, optical and electrical parameters of spray deposited ZnSe thin film with different substrate temperature.*" Eur. Phys. J. B **45**, 465-471 (2005)

2.M. Öztaş, M. Bedir, Ö. F. Bakkaloğlu and R. Ormancı.,*"Effect of Zn:Se Ratio on the Properties of Sprayed ZnSeThin Films."* Acta Physica Polonica A **107**, 525-534 (2005)

3. M. Bedir, M. Öztaş, R. Ormancı and Ö. F. Bakkaloğlu , "*The Effect of the Substrate Temperature of the Caracteristic Parameters of the Sprayed ZnSe Thin film*". TFD 22.Fizik Kongresi 14-17 Eylül 2004 Bodrum-Türkiye.